μl) were mixed with 100 μl of freshly prepared substrate solution (0.1% L-DOPA in phosphate-buffered saline) and incubated at 37 °C. The production of DOPAchrome was monitored by measuring the absorbance at 475 nm with a plate reader (Fluostar Galaxy) and corrected for auto-oxidation of L-DOPA.

Real-time RT-PCR Analysis—Real-time RT-PCR was performed as previously described (43) with some modifications. Total RNA was extracted from cells using an RNeasy kit according to the manufacturer's protocol. Samples (2.5 μg of RNA) were reverse-transcribed using a first-strand cDNA synthesis kit. Synthesized cDNA was used in real-time RT-PCR (Chromo 4 instrument (Bio-Rad)) experiments using iQ SYBR Green Supermix and analyzed with Opticon Monitor Software. Specificity was confirmed by electrophoretic analysis of the reaction products and by inclusion of template- or reverse transcriptase-free controls. To normalize the amount of total RNA present in each reaction, glyceraldehyde-3-phosphate dehydrogenase (GAPDH) cDNA was used as an internal standard.

Primers were designed using the Primer3 website. The primers used were (forward and reverse primers, respectively): tyrosinase, 5′-cctcctggcagatcatttgt-3′ and 5′-ggttttggctttgtcatggt-3′; *gapdh*, 5′-aactttggcattgtggaagg-3′ and 5′-acacattgggggtaggaaca-3′; *mitf*, 5′-ctagagcgcatggactttcc-3′ and 5′-acaagttcctggctgcagtt-3′.

siRNA Targeting of Genes—We used siRNA with the sequences of 5′-agcaguaccuuucuaccacdTdT-3′ and 5′-gugguagaaagguacugcudTdT-3′ as annealed oligonucleotides for repressing MITF expression. Cells were transfected with siRNA using HiPerFect transfection reagent according to the manufacturer's instructions. Non-silencing siRNA (5′-uucuccgaacgugucacgudTdT-3′ and 5′-acgugacacguucggagaadTdT-3′) was used as a negative control.

Luciferase Reporter Assay—The plasmid, pGL4-tyrosinase-luc (44), was a gift from Dr. M. Funaba (Kyoto University). The luciferase assay was performed as described previously (44, 45). Cells were transfected with 1 μg of each of the *Photinus pyralis* luciferase reporter plasmids (pGL4-tyrosinase-luc) and 0.125 μg of an internal standard plasmid bearing the *Renilla reniformis* luciferase reporter (pRL-SV40). *P. pyralis* luciferase activity in the cell extract was measured using the Dual Luciferase Assay System and then normalized for *Renilla reniformis* luciferase activity.

Co-immunoprecipitation Assay—Immunoprecipitation was carried out as described previously (46) with some modifications. Cells were harvested, lysed, and centrifuged. The antibody against HSP70 or MITF was added to the supernatant, and the samples were incubated for 12 h at 4 °C with rotation. Dynabeads Protein G was added and incubated for 2 h at 4 °C with rotation. Beads were washed four times, and proteins were eluted by boiling in SDS sample buffer.

Immunostaining Microscopy—After fixation with 4% paraformaldehyde, cells were incubated with antibody against HSP70 or MITF for overnight. Samples were further incubated with the respective secondary antibody. We acquired images with a confocal fluorescence microscope (Olympus FV500).

ChromatinImmunoprecipitationAssay—A chromatin immunoprecipitation assay was done as described previously (47) with some modifications. Cells were cross-linked with 1% formaldehyde for 10 min at 25 °C. After the addition of 125 mM (final concentration) glycine, cells were harvested and suspended in the lysis buffer (10 mM HEPES, 1.5 mM $MgCl_2$, 10 mM KCl, 0.5 mM dithiothreitol, 0.1% Nonidet P-40, and protease inhibitors). After 10 min of incubation on ice, cells were centrifuged to pellet the nuclei. Nuclei were then suspended in the nuclei lysis buffer (50 mM Tris/HCl (pH 8.1), 10 mM EDTA, 1% SDS, and protease inhibitors). Samples were sonicated 30 times for 10 *s* (to achieve an average fragment size of 0.5–1 kb). Immunoprecipitation was performed with magnetic beads that were coated with protein G and antibody against MITF or HSP70. Precipitates were washed, processed for DNA purification, and subjected to real time RT-PCR.

The primers used were (forward and reverse primers, respectively): tyrosinase promoter, 5′-gtctacttatgatctctaaatacaacaggcttg-3′ and 5′-tcatacaaaatctgcaccaataggttaatgagtg-3′; *gapdh*, 5′-acccagaagactgtggatgg-3′ and 5′-cacattgggggtaggaacac-3′.

In Vitro Transcription Assay—*In vitro* transcription assay was done as described (48) with some modifications. Nuclear extracts (5 μg protein) were incubated with DNA fragments containing the tyrosinase promoter and transcribed region (−270/+59) or the glucose-regulated protein (*grp78*) promoter and transcribed region (−304/+253) in the buffer containing 20 mM HEPES/KOH (pH 7.9), 100 mM KCl, 0.5 mM dithiothreitol, 1 mM EDTA, 20% glycerol, 0.4 mM ATP, 0.4 mM CTP, 0.4 mM UTP, 0.016 mM GTP, [α-^{32}P]GTP, and 4 mM $MgCl_2$ for 60 min at 30 °C. Isolated RNAs were resolved by electrophoresis on 15% polyacrylamide gel containing 7 M urea. The gel was dried and autoradiographed.

Assay for Melanin Production in Vivo—Animals were exposed to UVB irradiation with a double bank of UVB lamps (peak emission at 312 nm, VL-215LM lamp, Vilber Lourmat). The energy of the UV was monitored by radiometer sensor (UVX-31, UV Products). Skin reflective colorimetric measurements were assessed with a narrow-band simple reflectance meter (Mexameter MX18, Courage-Khazaka). The measurement was done for four parts of the skin, and the mean was calculated. The measurement area was 5 mm in diameter, and the instrument was calibrated using black and white calibration plates. Skin biopsies were harvested and processed for Fontana-Masson staining, as described (49).

Statistical Analysis—All values are expressed as the mean ± S.D. or S.E. Two-way analysis of variance followed by the Tukey test was used to evaluate differences between more than three groups. Differences were considered to be significant for values of $p < 0.05$.

RESULTS

Inhibition of Melanin Production by Expression of HSP70—As mentioned above, it has been reported that heat treatment of mouse melanoma cells (Mel-Ab) suppresses melanin production (35, 36). In this study we tested whether similar results are observed for a different mouse melanoma cell line (B16). Because UVB irradiation of B16 cells did not stimulate the melanin production (supplemental Fig. S1, *A* and *B*), we used either α-MSH or IBMX (which is a cAMP-elevating agent that acts through inhibition of phosphodiesterase) to mimic UV-stimu-

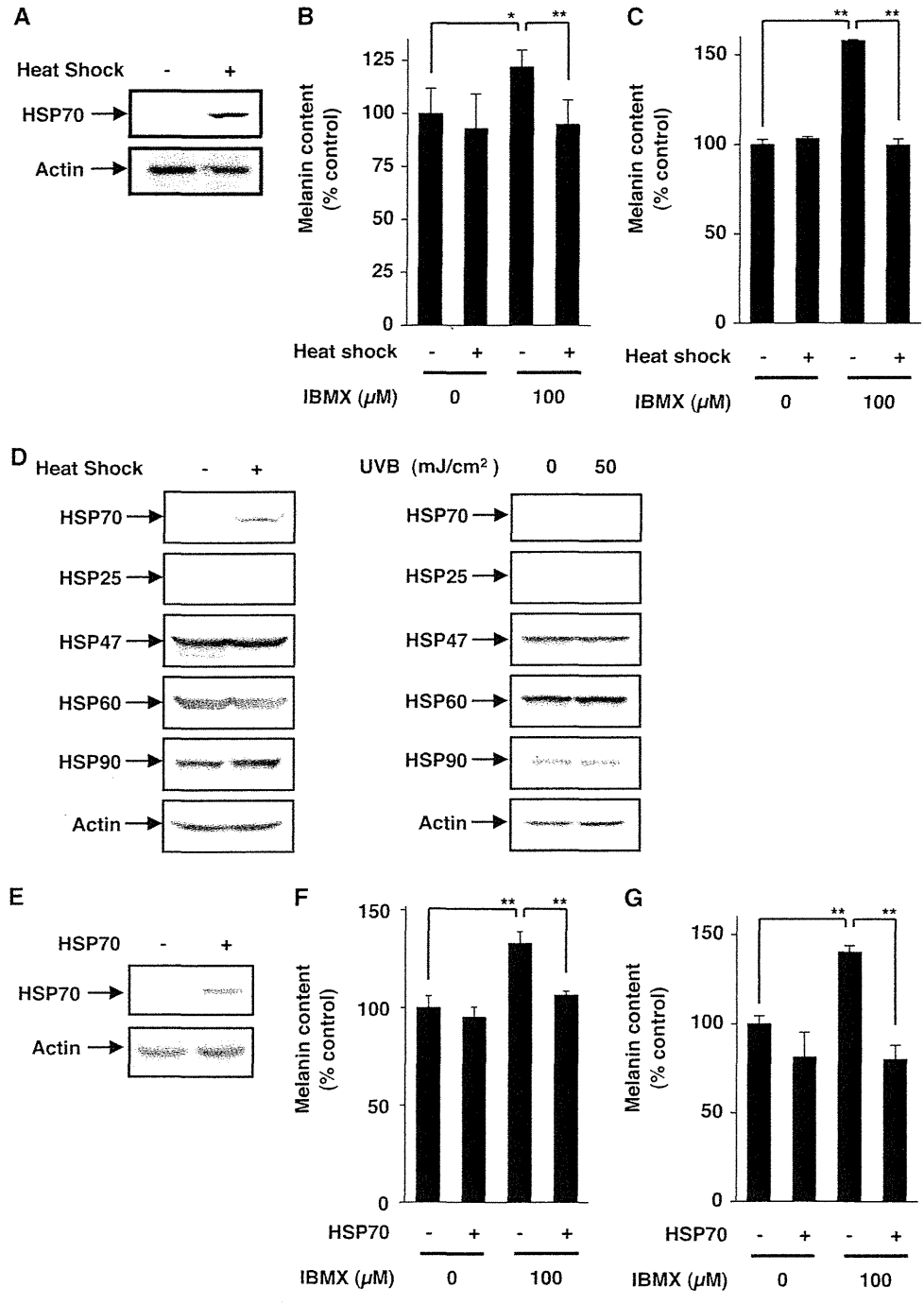

FIGURE 1. **Effect of heat treatment or overexpression of HSP70 on IBMX-stimulated melanin production.** B16 cells were incubated for 1.5 h at 42 °C (*Heat Shock* +) or 37 °C (*Heat Shock* −) then for 6 h at 37 °C and finally for 72 h at 37 °C with or without 100 μM IBMX (*A–C*). B16 cells were incubated for 1.5 h at 42 °C (*Heat Shock* +) or 37 °C (*Heat Shock* −) or irradiated with or without indicated doses of UVB and cultured for 24 h (*D*). HSP70-overexpressing B16 cells (*HSP70* +) and mock transfectant control cells (*HSP70* −) were incubated for 72 h with or without 100 μM IBMX (*E–G*). Whole cell extracts were analyzed by immunoblotting (*A*, *D*, and *E*). The amounts of melanin in the conditioned medium (*B* and *F*) or cell extract (*C* and *G*) were determined as described under "Experimental Procedures" and are expressed relative to the control. Values are given as the mean ± S.D. ($n = 3$). **, $p < 0.01$; *, $p < 0.05$.

lated melanin production *in vivo* and measured the amount of melanin in both the culture medium and cell extract. We confirmed that heat treatment (42 °C, 1.5 h) induced expression of HSP70 (Fig. 1*A*). As shown in Fig. 1, *B* and *C*, treatment of B16 cells with IBMX increased the melanin content in both fractions, and pretreatment of the cells with the heat shock suppressed this increase significantly, suggesting that the heat treatment inhibited IBMX-stimulated production of melanin. We also examined the effect of heat shock on melanin production in cells in which the production had been already activated by IBMX and found that the heat treatment inhibited the melanin production even under these conditions (supplemental Fig. S1, *C* and *D*). Similar results were observed for α-MSH-stimulated production of melanin (supplemental Fig. S1, *E* and *F*). As shown in Fig. 1*D*, this heat treatment also induced the expression of HSP25 weakly but did not induce the expression of other HSPs. We also found that UVB irradiation of B16 cells did not clearly affect the expression of HSPs (Fig. 1*D*).

We established a clone of B16 cells that stably overexpresses HSP70. The extent of expression of HSP70 in this clone is shown (Fig. 1*E*). We confirmed that this overexpression of HSP70 did not affect the cell growth (data not shown). IBMX- and α-MSH-dependent increases in the amount of melanin in the culture medium and cell extract were observed in the control clone but were not so apparent in the clone overexpressing HSP70 (Fig. 1, *F* and *G*, supplemental Fig. S1, *G* and *H*), showing that expression of HSP70 somehow inhibits the synthesis of melanin in B16 cells.

We also examined the effect of heat shock and/or UVB irradiation on melanin production with or without IBMX. As shown in supplemental Fig. S1, *I* and *J*, irradiation with UVB did not affect the melanin production with or without IBMX. UVB did not affect the melanin production even with simultaneous heat treatment (supplemental Fig. S1, *I* and *J*).

Mechanism for Inhibition of Melanin Production by Expression of HSP70—To understand the mechanisms governing inhibition of melanin production by expression of HSP70, we first examined tyrosinase activity. As shown in Fig. 2*A*, treatment of control cells with IBMX increased the tyrosinase activity in the cell extract as described previously (42), and this increase was not observed for cells

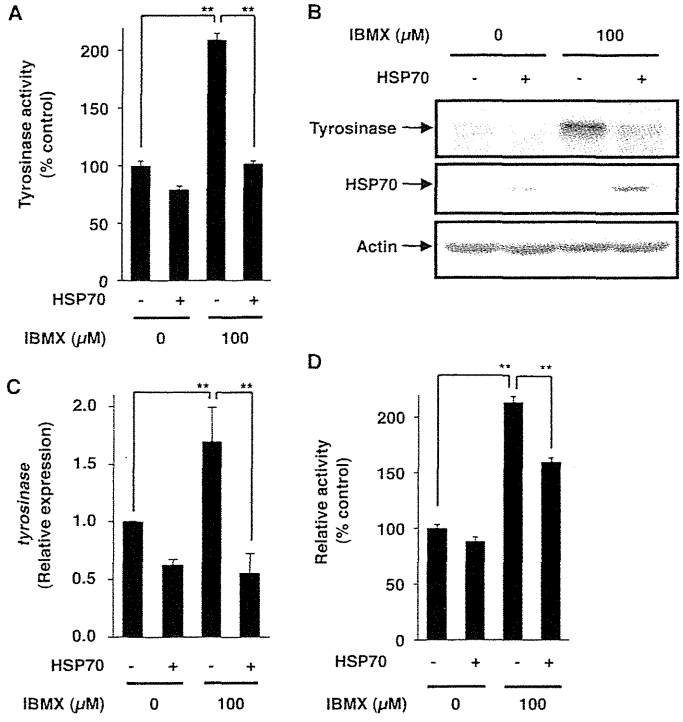

FIGURE 2. **Effect of overexpression of HSP70 on IBMX-stimulated activity and expression of tyrosinase.** HSP70-overexpressing B16 cells (*HSP70* +) and mock transfectant control cells (*HSP70* −) were incubated for 48 h with or without 100 μM IBMX (*A–C*). Tyrosinase activity was determined as described under "Experimental Procedures" and expressed relative to the control (*A*). Whole cell extracts were analyzed by immunoblotting as described in the legend of Fig. 1*B*. Total RNA was extracted and subjected to real-time RT-PCR using a specific primer for the tyrosinase gene. Values were normalized to *gapdh* gene expression and expressed relative to the control sample (*C*). HSP70-expressing B16 cells (*HSP70* +) and mock transfectant control cells (*HSP70* −) were transiently transfected with pRL-SV40 (internal control plasmid carrying the *R. reniformis* luciferase gene) and pGL4-tyrosinase-luc. After 24 h, the cells were incubated for 24 h with or without 100 μM IBMX. *P. pyralis* luciferase activity was measured and normalized for *R. reniformis* luciferase activity (*D*). Values are given as the mean ± S.D. ($n = 3$). **, $p < 0.01$.

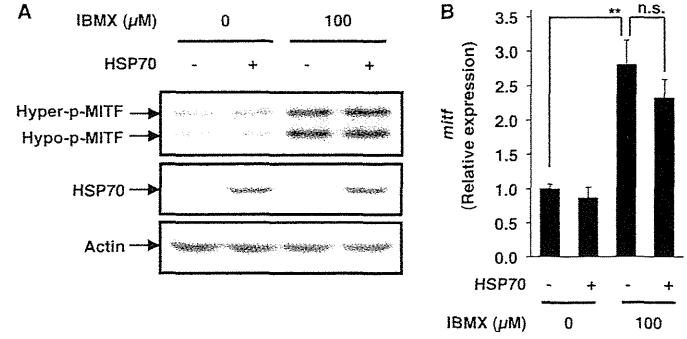

FIGURE 3. **Effect of overexpression of HSP70 on IBMX-stimulated expression of MITF.** HSP70-overexpressing B16 cells (*HSP70* +) or mock transfectant control cells (*HSP70* −) were incubated for 3 h with or without 100 μM IBMX (*A* and *B*). Whole cell extracts were analyzed by immunoblotting as described in the legend of Fig. 1. The bands representing the hyperphosphorylated (*Hyper-p*) and hypophosphorylated (*Hypo-p*) forms of MITF are shown (*A*). *mitf* mRNA expression was monitored as described in the legend of Fig. 2*B*. Values are given as the mean ± S.D. ($n = 3$). **, $p < 0.01$; *n.s.*, not significant.

overexpressing HSP70. We also examined the effect of IBMX and/or overexpression of HSP70 on the expression of tyrosinase. Treatment of cells with IBMX increased the level of tyrosinase, and this increase was suppressed in HSP70-overexpressing cells (Fig. 2*B*). Similar results were observed at the mRNA level, which was monitored by real-time RT-PCR (Fig. 2*C*), suggesting that expression of HSP70 inhibits transcription of the tyrosinase gene. To confirm this notion, we performed a luciferase reporter assay using a reporter plasmid where the promoter of the tyrosinase gene is inserted upstream of the luciferase gene. As shown in Fig. 2*D*, treatment of cells with IBMX increased luciferase activity in the cell extract, and the activity was significant lower in IBMX-treated HSP70-overexpressing cells than in the control cells, supporting the notion that expression of HSP70 inhibits the expression of tyrosinase at the level of transcription. Results similar to those in Fig. 2 were observed when heat treatment was used for induction of expression of HSP70 (supplemental Fig. S2, *A–D*).

As described in the introduction, MITF plays a central role in UV-induced expression of tyrosinase through its specific binding to the promoter of the tyrosinase gene (50). We examined the effect of IBMX and/or expression of HSP70 on the expression of MITF. As described previously (51), treatment of cells with IBMX increased the level of MITF (Fig. 3*A*). Surprisingly, expression of HSP70 did not affect the level of MITF irrespective of the presence of IBMX (Fig. 3*A*). Similar results were observed for mRNA expression (Fig. 3*B*). These results suggest that the inhibitory effect of HSP70 expression on the promoter activity of the tyrosinase gene is not mediated by alterations to the expression of MITF. It is known that MITF is activated by phosphorylation (50); however, the results in Fig. 3*A* also suggest that the level of phosphorylation (the ratio of the hyperphosphorylated form to the hypophosphorylated form of MITF) is not affected by expression of HSP70. We also examined the effect of heat shock on the level of MITF. As shown in supplemental Fig. S2, *E* and *F*, different from the case of overexpression of HSP70 (Fig. 3), heat treatment decreased the level of MITF and *mitf* mRNA.

To test whether MITF is required for HSP70-dependent regulation of the promoter activity of the tyrosinase gene, we examined the effect of siRNA for MITF on the promoter activity of the tyrosinase gene. As shown in Fig. 4, transfection with siRNA clearly inhibited the expression of MITF irrespective of the presence of IBMX and HSP70 overexpression. The siRNA suppressed IBMX-dependent activation of the promoter activity of the tyrosinase gene, and HSP70 overexpression did not affect the promoter activity in cells transfected with the siRNA (Fig. 4), suggesting that MITF plays an important role in the inhibitory effect of HSP70 on the promoter activity of the tyrosinase gene.

We also examined the expression of MITF-regulated genes other than the tyrosinase gene, such as tyrosinase-related protein 1 (Tyrp1), dopachrome tautomerase (Dct), and protein phosphatase methylesterase 1 (PmeI). Expression of these genes was enhanced by IBMX and this enhancement was suppressed in HSP70-overexpressing cells (supplemental Fig. S2, *G–I*).

Involvement of an Interaction between HSP70 and MITF in the Inhibitory Effect of HSP70 on Melanin Production—Based on the results mentioned above and the fact that HSP70 is a molecular chaperone modifying the activity of other proteins by its direct binding, we hypothesized that HSP70 interacts

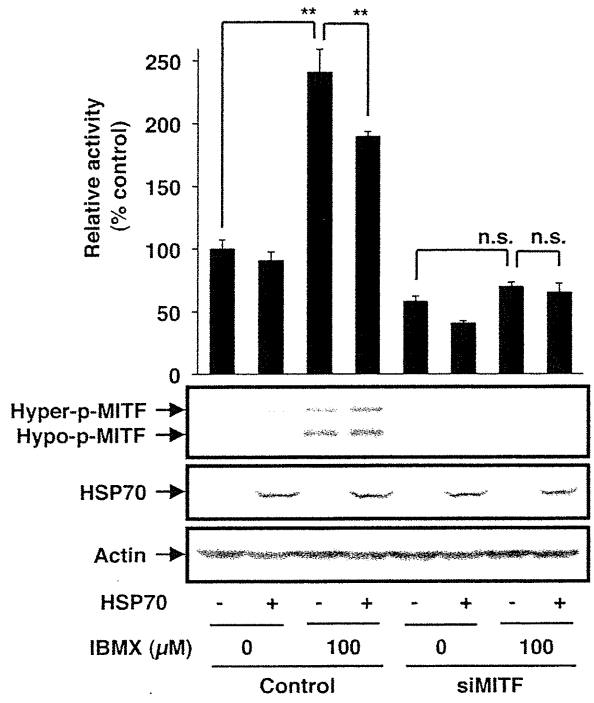

FIGURE 4. **Effect of siRNA for MITF on the IBMX-stimulated promoter activity of the tyrosinase gene.** HSP70-overexpressing B16 cells (*HSP70* +) or mock transfectant control cells (*HSP70* −) were transiently transfected with not only pRL-SV40 and pGL4-tyrosinase-luc but also with siRNA for MITF (*siMITF*) or non-silencing siRNA (*Control*). After 24 h, the cells were incubated for 24 h with or without 100 μM IBMX. Luciferase activity was measured and expressed as described in the legend of Fig. 2. Values are given as the mean ± S.D. ($n = 3$). **, $p < 0.01$; *n.s.*, not significant. Whole cell extracts were analyzed by immunoblotting as described in the legend of Fig. 3.

with MITF to modulate its effect on transcription of the tyrosinase gene. At first, we examined the physical interaction between HSP70 and MITF by a co-immunoprecipitation assay; we immunoprecipitated HSP70 and looked for the presence of MITF. Efficient precipitation of HSP70 was observed in a manner that was dependent on both the overexpression of HSP70 (Fig. 5*A*) and the specific antibody (data not shown). MITF was co-immunoprecipitated, and this co-immunoprecipitation was stimulated by overexpression of HSP70 (Fig. 5*A*). We also performed a reciprocal co-immunoprecipitation assay; we immunoprecipitated MITF and looked for the presence of HSP70. Efficient precipitation of MITF was observed in a manner that was dependent on the specific antibody (data not shown), and HSP70 was co-immunoprecipitated (Fig. 5*A*). These results suggest that HSP70 can physically interact with MITF.

We also examined the interaction using purified proteins. After incubation of purified glutathione *S*-transferase (GST)-fused MITF and HSP70, we precipitated GST-MITF and looked for the presence of HSP70. As shown in supplemental Fig. S3, precipitation of HSP70 was observed with full-length GST-MITF (GST-MITF-1) but not with GST alone, suggesting the direct interaction between MITF and HSP70. We also constructed a series of deletion mutants of GST-MITF to identify the domain of MITF responsible for its interaction with HSP70. Deletion of the N-terminal region of MITF (1–99 amino acid residues) diminished the interaction with HSP70, and the N-terminal fragment of MITF (1–99 amino acid residues) interacted with HSP70, suggesting that this region is responsible for the interaction (supplemental Fig. S3).

We then tested the co-localization of HSP70 and MITF by immunoblotting and immunostaining assays. As shown in Fig. 5*B*, MITF was detected in the nuclear extract irrespective of whether HSP70 was overexpressed, and HSP70 was also detected in the nuclear extract from cells overexpressing HSP70 but not in extract from control cells. These observations were confirmed by an immunostaining assay; MITF localized in the nucleus irrespective of the overexpression of HSP70, and HSP70 localized in the nucleus in a manner that was dependent on its overexpression (Fig. 5*C*). As a result, co-localization of HSP70 and MITF in the nucleus was observed in HSP70-overexpressing cells (see the *Merge panel* in Fig. 5*C*).

We then examined the effect of HSP70 overexpression on the specific binding of MITF to the promoter of the tyrosinase gene by chromatin immunoprecipitation assay. As shown in Fig. 6, DNA fragments containing the promoter of tyrosinase gene were precipitated with antibody against MITF more efficiently than control DNA fragments, suggesting that MITF specifically binds to the promoter of the tyrosinase gene in cells. We also found that this binding was stimulated by treatment of cells with IBMX, and HSP70 overexpression significantly inhibited this binding (Fig. 6). Results in Fig. 6 also suggest that HSP70 does not bind to the promoter of the tyrosinase gene so apparently in cells.

Finally, we examined the effect of HSP70 on the transcription of the tyrosinase gene in nuclear extract. DNA fragments containing the promoter region of the tyrosinase or *grp78* (control) were incubated with nuclear extract to promote the transcription, and transcripts were detected by autoradiography after separation on polyacrylamide gel electrophoresis. The band with the expected size was detected depending on the template DNA and nuclear extract (data not shown), showing that the band corresponds to the transcript of tyrosinase or *grp78*. The intensity of bands corresponding to the transcript of tyrosinase but not that of *grp78* increased by treatment of cells with IBMX (Fig. 7*A*). As shown in Fig. 7*A*, the intensity of band corresponding to the transcript of tyrosinase was lower with extracts prepared from HSP70-overexpressing cells treated with IBMX than those from control cells treated with IBMX. Such effect was not observed for the band corresponding to the transcript of *grp78* (Fig. 7*A*). Furthermore, the addition of purified HSP70 to extract prepared from control cells decrease the intensity of band corresponding to the transcript of tyrosinase but not of *grp78* (Fig. 7*B*). These results suggest that HSP70 directly suppresses the transcription of the tyrosinase.

Effect of Expression of HSP70 on UVB-induced Melanin Production in Vivo—Finally, we tested the *in vivo* relevance of our *in vitro* results using transgenic mice expressing HSP70. The transgenic mice and wild-type mice were exposed to UVB irradiation for 8 days, and the melanin content was estimated by Fontana-Masson staining of sections or by a narrow-band simple reflectance meter (Mexameter). For this we used the tail skin because murine tail skin resembles human skin, as epidermal melanocytes are present and UV-dependent melanin production has been observed (52). We confirmed the overexpression of HSP70 in the skin of the transgenic mice by an

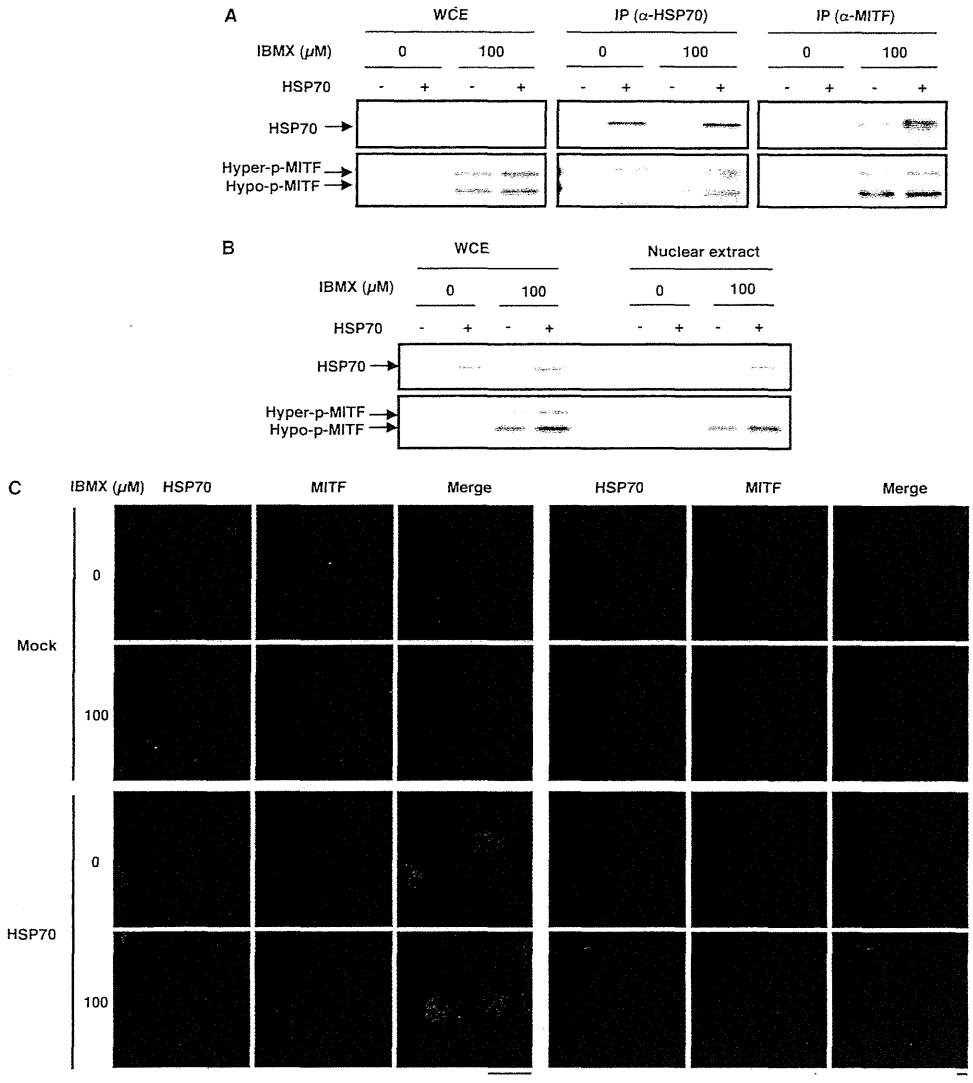

FIGURE 5. **Physical interaction between MITF and HSP70 and their intracellular co-localization.** HSP70-overexpressing B16 cells (*HSP70* +) or mock transfectant control cells (*HSP70* −) were incubated for 3 h with or without 100 μM IBMX (*A–C*), and whole cell extracts (*WCE*) were prepared (*A* and *B*). WCE were immunoprecipitated with antibodies against HSP70 (*IP (α-HSP70)*) or those against MITF (*IP (α-MITF)*) (*A*), or nuclear extracts were prepared from whole cell extracts (*B*). Each fraction was analyzed by immunoblotting as described in the legend of Fig. 1 (*A* and *B*). After fixation, samples were incubated with antibody against HSP70 or MITF. After incubation with the respective secondary antibody, cells were inspected using fluorescence microscopy. The *left three panels* are the magnified image of the *right three panels*. *Scale bar*, 20 μm (*C*).

immunoblotting assay (data not shown). As shown in Fig. 8*A*, an increase in melanin staining at the basal layer of the epidermis (the dermal/epidermal border) was observed in the wild-type mice after UVB irradiation, but this increase was not so obvious in sections prepared from the transgenic mice expressing HSP70. Measurement of melanin content by a Mexameter also showed that the melanin content was lower in the UVB-treated transgenic mice expressing HSP70 than in the wild-type controls (Fig. 8*B*). We also found that heat treatment of tail skin caused overexpression of HSP70 and a lower level of melanin content after irradiation with UVB (supplemental Fig. S4).

DISCUSSION

It has been reported that heat treatment of mouse melanoma cells (Mel-Ab) suppresses melanin production; however, it is not clear whether up-regulation of expression of HSPs is involved in this phenomenon because an HSP-independent mechanism such as activation of extracellular signal-regulated kinase (ERK) and inhibition of p38 mitogen-activated protein kinase (p38 MAPK) has been proposed to be responsible for this phenomenon (35, 36). In this study we confirmed the inhibitory effect of heat treatment on melanin production in another type of mouse melanoma (B16) and showed that artificial overexpression of HSP70 also suppresses melanin production, suggesting that up-regulation of HSP70 expression is involved in the inhibitory effect of heat treatment on melanin production. Other mechanisms, such as activation of ERK and inhibition of p38 MAPK, may also contribute to the inhibitory effect of heat treatment on melanin production (35, 36). Furthermore, a decrease in the level of MITF after heat treatment (supplemental Fig. S2, *E* and *F*) should be involved in the inhibitory effect of heat treatment on melanin production.

Because HSPs are known to affect the intracellular traffic of vesicles, it is possible that expression of HSP70 affects the intracellular traffic of melanosomes, resulting in alterations to the amount of melanin in the culture medium. However, as well as heat treatment, artificial overexpression of HSP70 decreased the amount of melanin not only in the culture medium but also in cell extracts. This suggests that the decrease in the amount of melanin in the culture medium cannot be simply explained by the alteration of intracellular traffic of melanosomes and that synthesis of melanin by melanosomes is suppressed by overexpression of HSP70. In fact, we found that the activity and expression of tyrosinase (a rate-limiting enzyme in the synthesis of melanin) are suppressed in cells overexpressing HSP70. It is well known that the activity of tyrosinase is regulated mainly at the level of transcription, and we found by real-time RT-PCR analysis and luciferase reporter assay that the transcriptional activity of the tyrosinase gene is suppressed in cells overexpressing HSP70. Furthermore, in cells transfected with siRNA specific for MITF (a key transcription factor regulating the transcription of the tyrosinase gene), overexpression of HSP70 did not affect the promoter activity of the tyrosinase gene, suggesting that MITF plays an important role in HSP70-dependent regulation of the transcription of the tyrosinase gene.

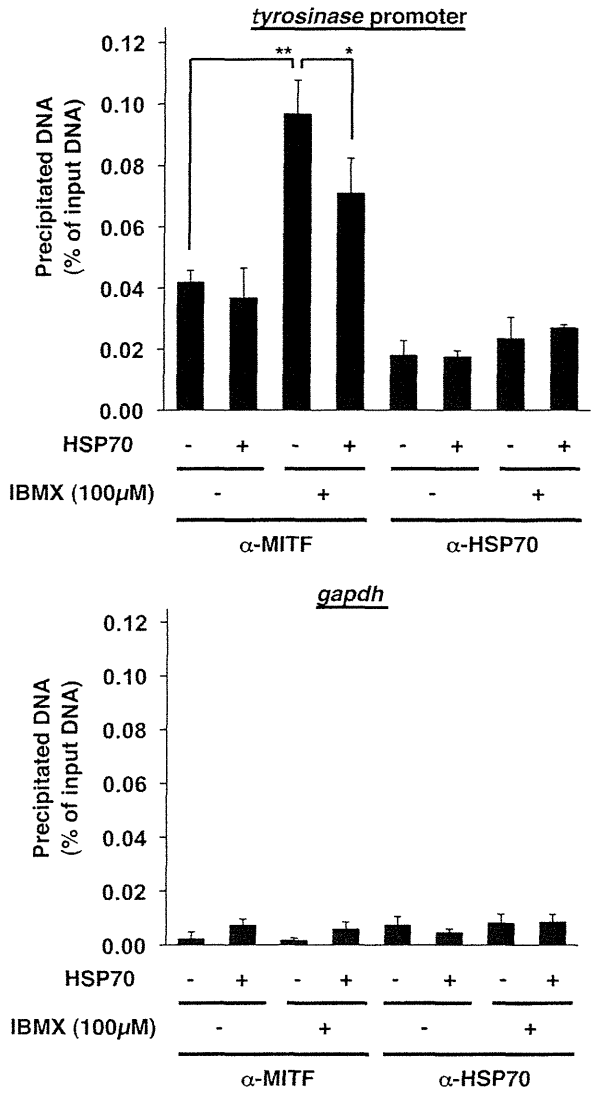

FIGURE 6. **The binding of MITF to the promoter of the tyrosinase gene in cells.** HSP70-overexpressing B16 cells (*HSP70* +) and mock transfectant control cells (*HSP70* −) were incubated for 24 h with or without 100 μM IBMX. Whole cell extracts were immunoprecipitated with an antibody against MITF or HSP70. DNA fractions were prepared from the immunoprecipitated samples, and whole cell extracts and subjected to real time RT-PCR with specific primer sets for the tyrosinase promoter (*upper panel*) and *gapdh* gene (*lower panel*). Values are expressed relative to the input DNA (whole cell extracts) and are given as mean ± S.D. ($n = 3$). **, $p < 0.01$; *, $p < 0.05$.

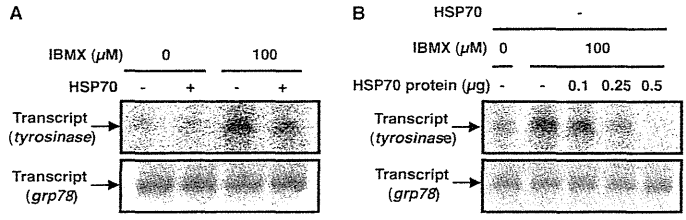

FIGURE 7. **Effect of HSP70 on the transcription of the tyrosinase gene in nuclear extract.** HSP70-overepressing B16 cells (*HSP70* +) or mock transfectant control cells (*HSP70* −) were incubated for 3 h with or without 100 μM IBMX. Nuclear extracts were prepared and incubated with DNA fragments containing the tyrosinase or *grp78* promoter region in the presence (*B*) or absence (*A*) of indicated amounts of purified HSP70 (*B*). Isolated RNAs were electrophoresed on a 15% polyacrylamide gel and autoradiographed.

The pathway of activation of adenylate cyclase followed by an increase in the intracellular cAMP level and activation of protein kinase A/cAMP response element-binding protein has

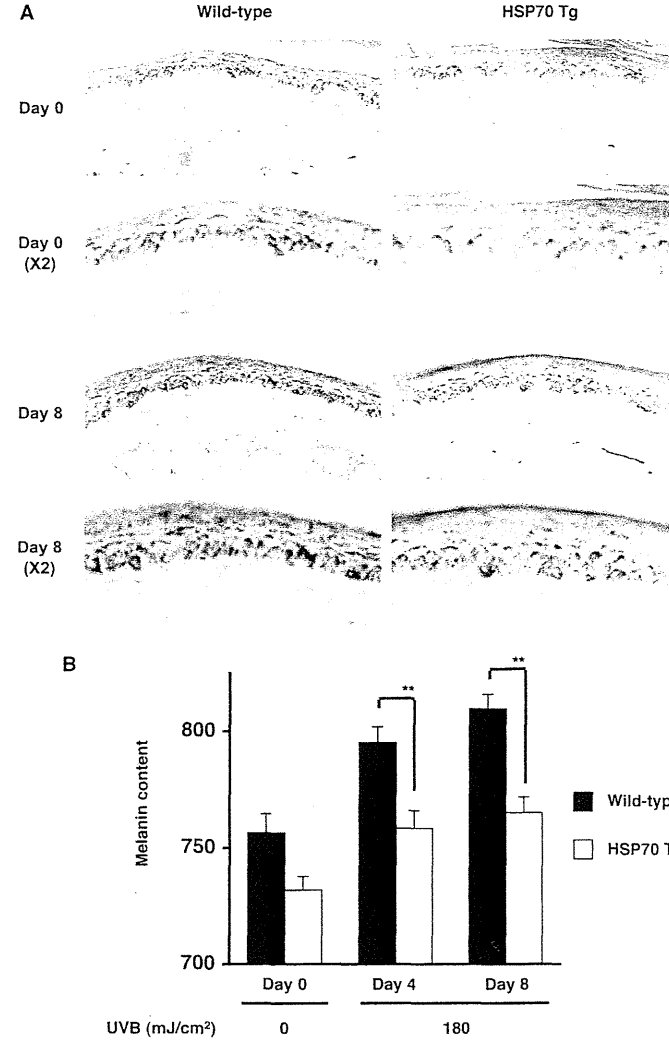

FIGURE 8. **Effect of overexpression of HSP70 on UVB-induced melanin production in the skin *in vivo*.** Transgenic mice expressing HSP70 (*HSP70 Tg*) and wild-type mice (C57/BL6) were irradiated with 180 mJ/cm² UVB once per 2 days for 8 days (totally 4 times) (*A* and *B*). Sections were prepared from the tail skin and subjected to Fontana-Masson staining (*A*). The amount of melanin in the tail skin was measured as described under "Experimental Procedures." Values are given as the mean ± S.E. ($n = 17$). **, $p < 0.01$ (*B*).

been proposed to play an important role in the UV-induced expression of tyrosinase mainly through induction of MITF expression (7). In this study we have confirmed that IBMX up-regulates the expression of MITF. However, surprisingly, overexpression of HSP70 did not affect this up-regulation. Thus, we propose an alternative mechanism for the inhibitory effect of HSP70 on expression of the tyrosinase gene; HSP70 directly binds to MITF in the nucleus and inhibits its specific binding to the promoter of the tyrosinase gene. This is based on the following results; HSP70 can physically interact with MITF (co-immunoprecipitation assay), overexpressed HSP70 co-localized with MITF in the nucleus (co-immunostaining assay), overexpression of HSP70 inhibited the specific binding of MITF to the promoter of the tyrosinase gene (chromatin immunoprecipitation assay), and HSP70 inhibited the transcription of the tyrosinase gene in nuclear extract.

On the other hand, it has been reported that heat treatment suppresses the promoter activity of the *mitf* gene and sup-

presses the expression of MITF through inhibition of protein phosphatase 2A and ERK activation (36). Furthermore, it was suggested that heat treatment suppresses the activity of tyrosinase through p38 MAPK suppression (35). Thus, the inhibitory effect of heat treatment on melanin production would be mediated not only by expression of HSP70 but also by ERK activation and p38 MAPK suppression.

We also suggest that the expression of HSP70 suppresses UVB-induced synthesis of melanin *in vivo*; transgenic mice expressing HSP70 showed a smaller UV-dependent increase in the melanin content of the skin than wild-type mice. We have considered that the mechanism that is suggested by our *in vitro* studies is responsible for this *in vivo* phenomenon. Because hypopigmenting reagents are useful as drugs and cosmetics, a number of compounds that inhibit tyrosinase and/or MITF have been discovered; however, most of their cosmetic and pharmaceutical applications have not been successful due to skin irritation and permanent depigmentation (53). This seems to be due to the fact that UV-induced melanogenesis has a protective role against UV-induced skin damage. Based on the results of this study, we propose that non-toxic HSP70-inducers could be cosmetically and pharmaceutically beneficial because HSP70 protects keratinocytes from UV-induced cell damage both *in vitro* and *in vivo* (24, 29–33). Furthermore, human HSP70 has been reported to stimulate deoxyribonucleic acid base excision repair by its direct binding to human AP endonuclease and uracil DNA glycosylase (54). In *E. coli*, an HSP70 homologue (DnaK) stimulates the nucleotide excision repair of damaged DNA by maintaining repair proteins in their properly folded state (55), suggesting that human HSP70 may also stimulate nucleotide excision repair. We recently found that expression of HSP70 suppresses UV-induced DNA damage and stimulates its repair process at the skin in mice (56). Other beneficial effects of HSP70, such as stimulation of wound-healing at the skin and anti-aging activity have also been suggested (57–60). Furthermore, because recent reports suggest that MITF is an oncogene and its activation is involved in the progression of melanoma (61), the inhibitory effect of HSP70 on MITF would be beneficial for the prevention of UV-induced melanoma. We have already screened for non-toxic HSP70 inducers from natural products and found that some of their HSP-inducing activities were more potent than geranylgeranylacetone (62). We hope to develop some of these as whitening cosmetics or drugs for melanin-related diseases.

Acknowledgments—We thank Drs. C. E. Angelidis and G. N. Pagoulatos (University of Ioannina) or Dr. M. Funaba (Kyoto University) for generously providing transgenic mice expressing HSP70 or a plasmids, respectively.

REFERENCES

1. Rabe, J. H., Mamelak, A. J., McElgunn, P. J., Morison, W. L., and Sauder, D. N. (2006) *J. Am. Acad. Dermatol.* **55,** 1–19
2. Svobodova, A., Walterova, D., and Vostalova, J. (2006) *Biomed. Pap. Med. Fac. Univ. Palacky Olomouc. Czech Repub.* **150,** 25–38
3. McMillan, T. J., Leatherman, E., Ridley, A., Shorrocks, J., Tobi, S. E., and Whiteside, J. R. (2008) *J. Pharm. Pharmacol.* **60,** 969–976
4. Shorrocks, J., Paul, N. D., and McMillan, T. J. (2008) *J. Invest. Dermatol.* **128,** 685–693
5. Douki, T., Reynaud-Angelin, A., Cadet, J., and Sage, E. (2003) *Biochemistry* **42,** 9221–9226
6. Matsumura, Y., and Ananthaswamy, H. N. (2004) *Toxicol. Appl. Pharmacol.* **195,** 298–308
7. Buscà, R., and Ballotti, R. (2000) *Pigment Cell Res.* **13,** 60–69
8. Yamaguchi, Y., Brenner, M., and Hearing, V. J. (2007) *J. Biol. Chem.* **282,** 27557–27561
9. D'Orazio, J. A., Nobuhisa, T., Cui, R., Arya, M., Spry, M., Wakamatsu, K., Igras, V., Kunisada, T., Granter, S. R., Nishimura, E. K., Ito, S., and Fisher, D. E. (2006) *Nature* **443,** 340–344
10. Costin, G. E., and Hearing, V. J. (2007) *FASEB J.* **21,** 976–994
11. Miyamura, Y., Coelho, S. G., Wolber, R., Miller, S. A., Wakamatsu, K., Zmudzka, B. Z., Ito, S., Smuda, C., Passeron, T., Choi, W., Batzer, J., Yamaguchi, Y., Beer, J. Z., and Hearing, V. J. (2007) *Pigment Cell Res.* **20,** 2–13
12. Agar, N., and Young, A. R. (2005) *Mutat. Res.* **571,** 121–132
13. Sturm, R. A., Duffy, D. L., Box, N. F., Chen, W., Smit, D. J., Brown, D. L., Stow, J. L., Leonard, J. H., and Martin, N. G. (2003) *Pigment Cell Res.* **16,** 266–272
14. Kobayashi, N., Nakagawa, A., Muramatsu, T., Yamashina, Y., Shirai, T., Hashimoto, M. W., Ishigaki, Y., Ohnishi, T., and Mori, T. (1998) *J. Invest. Dermatol.* **110,** 806–810
15. Bustamante, J., Bredeston, L., Malanga, G., and Mordoh, J. (1993) *Pigment Cell Res.* **6,** 348–353
16. Morimoto, R. I., and Santoro, M. G. (1998) *Nat. Biotechnol.* **16,** 833–838
17. Tanaka, K., Namba, T., Arai, Y., Fujimoto, M., Adachi, H., Sobue, G., Takeuchi, K., Nakai, A., and Mizushima, T. (2007) *J. Biol. Chem.* **282,** 23240–23252
18. Tanaka, K., Tsutsumi, S., Arai, Y., Hoshino, T., Suzuki, K., Takaki, E., Ito, T., Takeuchi, K., Nakai, A., and Mizushima, T. (2007) *Mol. Pharmacol.* **71,** 985–993
19. Asano, T., Tanaka, K., Yamakawa, N., Adachi, H., Sobue, G., Goto, H., Takeuchi, K., and Mizushima, T. (2009) *J. Pharmacol. Exp. Ther.* **330,** 458–467
20. Suemasu, S., Tanaka, K., Namba, T., Ishihara, T., Katsu, T., Fujimoto, M., Adachi, H., Sobue, G., Takeuchi, K., Nakai, A., and Mizushima, T. (2009) *J. Biol. Chem.* **284,** 19705–19715
21. Hirakawa, T., Rokutan, K., Nikawa, T., and Kishi, K. (1996) *Gastroenterology* **111,** 345–357
22. Ohkawara, T., Nishihira, J., Takeda, H., Miyashita, K., Kato, K., Kato, M., Sugiyama, T., and Asaka, M. (2005) *Scand. J. Gastroenterol.* **40,** 1049–1057
23. Ohkawara, T., Nishihira, J., Takeda, H., Katsurada, T., Kato, K., Yoshiki, T., Sugiyama, T., and Asaka, M. (2006) *Int. J. Mol. Med.* **17,** 229–234
24. Wilson, N., McArdle, A., Guerin, D., Tasker, H., Wareing, P., Foster, C. S., Jackson, M. J., and Rhodes, L. E. (2000) *J. Cutan. Pathol.* **27,** 176–182
25. Morris, S. D. (2002) *Clin. Exp. Dermatol.* **27,** 220–224
26. Jonak, C., Klosner, G., and Trautinger, F. (2006) *Int. J. Cosmet. Sci.* **28,** 233–241
27. Trautinger, F., Kokesch, C., Klosner, G., Knobler, R. M., and Kindas-Mügge, I. (1999) *Exp. Dermatol.* **8,** 187–192
28. Allanson, M., and Reeve, V. E. (2004) *J. Invest. Dermatol.* **122,** 1030–1036
29. Trautinger, F. (2001) *J. Photochem. Photobiol. B* **63,** 70–77
30. Trautinger, F., Kindås-Mügge, I., Barlan, B., Neuner, P., and Knobler, R. M. (1995) *J. Invest. Dermatol.* **105,** 160–162
31. Park, K. C., Kim, D. S., Choi, H. O., Kim, K. H., Chung, J. H., Eun, H. C., Lee, J. S., and Seo, J. S. (2000) *Arch. Dermatol. Res.* **292,** 482–487
32. Maytin, E. V., Wimberly, J. M., and Kane, K. S. (1994) *J. Invest. Dermatol.* **103,** 547–553
33. Kwon, S. B., Young, C., Kim, D. S., Choi, H. O., Kim, K. H., Chung, J. H., Eun, H. C., Park, K. C., Oh, C. K., and Seo, J. S. (2002) *J. Dermatol. Sci.* **28,** 144–151
34. Trautinger, F., Knobler, R. M., Hönigsmann, H., Mayr, W., and Kindås-Mügge, I. (1996) *J. Invest. Dermatol.* **107,** 442–443
35. Kim, D. S., Park, S. H., Kwon, S. B., Na, J. I., Huh, C. H., and Park, K. C. (2007) *Arch. Pharm. Res.* **30,** 581–586
36. Kim, D. S., Park, S. H., Kwon, S. B., Youn, S. W., Park, E. S., and Park, K. C.

(2005) *Cell. Signal.* **17,** 1023–1031
37. Fujimoto, M., Takaki, E., Hayashi, T., Kitaura, Y., Tanaka, Y., Inouye, S., and Nakai, A. (2005) *J. Biol. Chem.* **280,** 34908–34916
38. Hoshino, T., Tsutsumi, S., Tomisato, W., Hwang, H. J., Tsuchiya, T., and Mizushima, T. (2003) *J. Biol. Chem.* **278,** 12752–12758
39. Bradford, M. M. (1976) *Anal. Biochem.* **72,** 248–254
40. Kim, K. S., Kim, J. A., Eom, S. Y., Lee, S. H., Min, K. R., and Kim, Y. (2006) *Pigment Cell Res.* **19,** 90–98
41. Lei, T. C., Virador, V. M., Vieira, W. D., and Hearing, V. J. (2002) *Anal. Biochem.* **305,** 260–268
42. Yang, J. Y., Koo, J. H., Song, Y. G., Kwon, K. B., Lee, J. H., Sohn, H. S., Park, B. H., Jhee, E. C., and Park, J. W. (2006) *Acta Pharmacol. Sin.* **27,** 1467–1473
43. Mima, S., Tsutsumi, S., Ushijima, H., Takeda, M., Fukuda, I., Yokomizo, K., Suzuki, K., Sano, K., Nakanishi, T., Tomisato, W., Tsuchiya, T., and Mizushima, T. (2005) *Cancer Res.* **65,** 1868–1876
44. Murakami, M., Iwata, Y., and Funaba, M. (2007) *Mol. Cell Biochem.* **303,** 251–257
45. Namba, T., Homan, T., Nishimura, T., Mima, S., Hoshino, T., and Mizushima, T. (2009) *J. Biol. Chem.* **284,** 4158–4167
46. Hoshino, T., Nakaya, T., Araki, W., Suzuki, K., Suzuki, T., and Mizushima, T. (2007) *Biochem. J.* **402,** 581–589
47. Takehara, M., Makise, M., Takenaka, H., Asano, T., and Mizushima, T. (2008) *Biochem. J.* **413,** 535–543
48. Dignam, J. D., Lebovitz, R. M., and Roeder, R. G. (1983) *Nucleic Acids Res.* **11,** 1475–1489
49. Ito, T., Ito, N., Saathoff, M., Bettermann, A., Takigawa, M., and Paus, R. (2005) *Br. J. Dermatol.* **152,** 623–631
50. Levy, C., Khaled, M., and Fisher, D. E. (2006) *Trends Mol. Med.* **12,** 406–414
51. Park, H. Y., Wu, C., Yonemoto, L., Murphy-Smith, M., Wu, H., Stachur, C. M., and Gilchrest, B. A. (2006) *Biochem. J.* **395,** 571–578
52. Cui, R., Widlund, H. R., Feige, E., Lin, J. Y., Wilensky, D. L., Igras, V. E., D'Orazio, J., Fung, C. Y., Schanbacher, C. F., Granter, S. R., and Fisher, D. E. (2007) *Cell* **128,** 853–864
53. Ando, H., Kondoh, H., Ichihashi, M., and Hearing, V. J. (2007) *J. Invest. Dermatol.* **127,** 751–761
54. Bases, R. (2006) *Cell Stress Chaperones* **11,** 240–249
55. Zou, Y., Crowley, D. J., and Van Houten, B. (1998) *J. Biol. Chem.* **273,** 12887–12892
56. Matsuda, M., Hoshino, T., Yamashita, Y., Tanaka, K., Maji, D., Sato, K., Adachi, H., Sobue, G., Ihn, H., Funasaka, Y., and Mizushima, T. (2010) *J. Biol. Chem.* **285,** 5848–5858
57. Simon, M. M., Reikerstorfer, A., Schwarz, A., Krone, C., Luger, T. A., Jäättelä, M., and Schwarz, T. (1995) *J. Clin. Invest.* **95,** 926–933
58. Gutsmann-Conrad, A., Heydari, A. R., You, S., and Richardson, A. (1998) *Exp. Cell Res.* **241,** 404–413
59. Kimura, K., Tanaka, N., Nakamura, N., Takano, S., and Ohkuma, S. (2007) *J. Biol. Chem.* **282,** 5910–5918
60. Rattan, S. I. (1998) *Biochem. Mol. Biol. Int.* **45,** 753–759
61. Garraway, L. A., Widlund, H. R., Rubin, M. A., Getz, G., Berger, A. J., Ramaswamy, S., Beroukhim, R., Milner, D. A., Granter, S. R., Du, J., Lee, C., Wagner, S. N., Li, C., Golub, T. R., Rimm, D. L., Meyerson, M. L., Fisher, D. E., and Sellers, W. R. (2005) *Nature* **436,** 117–122
62. Yamashita, Y., Hoshino, T., Matsuda, M., Kobayashi, C., Tominaga, A., Nakamura, Y., Nakashima, K., Yokomizo, K., Ikeda, T., Mineda, K., Maji, D., Niwano, Y., and Mizushima, T. (2010) *Exp. Dermatol.*, in press

Cell Death and Differentiation (2010) 17, 1882–1895

www.nature.com/cdd

Induction of EMT-like phenotypes by an active metabolite of leflunomide and its contribution to pulmonary fibrosis

T Namba[1], K-I Tanaka[1], Y Ito[1], T Hoshino[1], M Matoyama[1], N Yamakawa[1], Y Isohama[1], A Azuma[2] and T Mizushima*[,1]

Drug-induced interstitial lung disease (ILD), particularly pulmonary fibrosis, is a serious clinical concern and myofibroblasts have been suggested to have a major role, with it recently being revealed that some of these myofibroblasts are derived from lung epithelial cells through epithelial–mesenchymal transition (EMT). In this study, we examined the EMT-inducing abilities of drugs known to induce ILD clinically. EMT-like phenotypes were induced by A771726, an active metabolite of leflunomide having an inhibitory effect on dihydroorotate dehydrogenase (DHODH). Smad-interacting protein 1 (a transcription factor regulating EMT) and the Notch-signaling pathway but not transforming growth factor-β was shown to be involved in A771726-induced EMT-like phenotypes. When the cultures were supplemented with exogenous uridine, the A771726-induced EMT-like phenotypes and activation of the Notch-signaling pathway disappeared. Similarly, an A771726 analog without inhibitory activity on DHODH produced no induction, suggesting that this process is mediated through the inhibition of DHODH. *In vivo*, administration of leflunomide stimulated bleomycin-induced EMT-like phenomenon in pulmonary tissue, and exacerbated bleomycin-induced pulmonary fibrosis, both of which were suppressed by coadministration of uridine. Taken together, these findings suggest that leflunomide-dependent exacerbation of bleomycin-induced pulmonary fibrosis is mediated by stimulation of EMT of lung epithelial cells, providing the first evidence that drug-induced pulmonary fibrosis involves EMT of these cells.
Cell Death and Differentiation (2010) **17,** 1882–1895; doi:10.1038/cdd.2010.64; published online 21 May 2010

Interstitial lung disease (ILD), in particular interstitial pneumonia associated with pulmonary fibrosis, is a devastating chronic lung condition with poor prognosis. Pulmonary fibrosis progresses insidiously and slowly, with acute exacerbation of interstitial pneumonia being a highly lethal clinical event. Furthermore, the mortality rate for pulmonary fibrosis is increasing.[1,2] Although most cases of pulmonary fibrosis are idiopathic, some are due to drug side effects (drug-induced pulmonary fibrosis). For example, the antitumor drugs imatinib and gefitinib, as well as the antirheumatoid arthritis drugs leflunomide and methotrexate, are known to induce ILD (pulmonary fibrosis). This is cause for serious clinical concern, as it can lead to patient death, thereby restricting the therapeutic use of these drugs.[3–5] Unfortunately, the etiology of drug-induced ILD (pulmonary fibrosis) is not yet understood and, as a result, an appropriate animal model has not yet been established. Although the bleomycin-induced pulmonary fibrosis animal model mimics some characteristics of human pulmonary fibrosis,[6] it remains unclear whether drugs known to induce ILD clinically exacerbate bleomycin-induced effects. Therefore, understanding the mechanism governing drug-induced ILD (pulmonary fibrosis) and developing a viable animal model are important to establish not only a clinical protocol for its treatment but also an assay system that will facilitate screening to eliminate candidate drugs with the potential to produce this type of side effect.

It is now believed that pulmonary fibrosis is induced by repeated epithelial cell damage and abnormal wound repair and remodeling, resulting in abnormal deposition of extracellular matrix (ECM) proteins, such as collagen. Cytokines, in particular transforming growth factor (TGF)-β_1, have been reported to have an important role in pulmonary fibrosis.[7] Inflammation, particularly that mediated by TGF-β_1 and reactive oxygen species is involved in repeated lung epithelial cell damage.[8] On the other hand, an increase in lung myofibroblasts has been suggested to have an important role in abnormal wound repair and remodeling.[9] Myofibroblasts extensively produce and secrete ECM proteins,[9] and are involved in abnormal wound repair and remodeling through various mechanisms, including deregulation of the balance between matrix metallopeptidases (MMPs) and tissue inhibitors of MMPs (TIMPs).[10] It was previously believed that the

[1]Graduate School of Medical and Pharmaceutical Sciences, Kumamoto University, Kumamoto 862-0973, Japan and [2]Division of Respiratory, Department of Internal Medicine, Infection and Oncology, Nippon Medical School, Tokyo 113-8602, Japan
*Corresponding author: T Mizushima, Graduated School of Medical and Pharmaceutical Sciences, Kumamoto University, 5-1 Oe-honmachi, Kumamoto 862-0973, Japan. Tel/Fax: +81 96 371 4323; E-mail: mizu@gpo.kumamoto-u.ac.jp
Keywords: EMT; leflunomide; pulmonary fibrosis
Abbreviations: 6-MP, 6-mercaptopurine; α-SMA, α-smooth muscle actin; BSA, bovine serum albumin; CTGF, connective tissue growth factor; DAPI, 4,6-diamino-2-phenylindole; DAPT, *N*-[*N*-(3,5-difluorophenacetyl-L-alanyl)]-*S*-phenylglycine t-butyl ester; DHODH, dihydroorotate dehydrogenase; DMBA, 4-(dimethylamino)-benzaldehyde; Dll-1, Delta-like 1; ECM, extracellular matrix; EMT, epithelial–mesenchymal transition; FBS, fetal bovine serum; ILD, interstitial lung disease; MMP, matrix metallopeptidase; NICD, Notch intracellular domain; proSP-C, precursor of surfactant protein-C; ISIP-1, Smad-interacting protein 1; TIMP, tissue inhibitor of matrix metalloprotease; TGF, transforming growth factor
Received 07.12.09; revised 08.4.10; accepted 19.4.10; Edited by RA Knight; published online 21.5.10

origin of myofibroblasts is solely peribronchiolar and perivascular fibroblasts that transdifferentiate to myofibroblasts in response to various stimuli, in particular TGF-β_1.[11] However, recently, it was shown that lung epithelial cells undergo epithelial–mesenchymal transition (EMT) to become myofibroblasts after treatment with TGF-β_1 *in vitro*.[12,13] The EMT of lung epithelial cells also seems to be induced in the lungs of pulmonary fibrosis patients and bleomycin-treated animals.[12,14] Furthermore, inhibition of EMT by knockout of the *integrin-α3* gene has been shown to suppress bleomycin-induced pulmonary fibrosis in mice.[15] These results suggest that some of the lung myofibroblasts in pulmonary fibrosis patients originate from lung epithelial cells through the EMT, and that EMT has an important role in the pathogenesis of the condition, including that induced by drugs. However, the involvement of EMT in drug-induced pulmonary fibrosis has not previously been examined.

Leflunomide, one of a number of newly developed disease-modifying antirheumatic drugs,[16,17] suppresses the cell-cycle progression of T lymphocytes and other types of cells by inhibiting mitochondrial dihydroorotate dehydrogenase (DHODH), which is the fourth enzyme in the *de novo* synthesis of pyrimidine.[18] This mechanism is supported by the observation that the inhibitory effect of leflunomide on cell growth is canceled by supplementing the cultures with exogenous uridine, which is a substrate of the salvage pathway of pyrimidine synthesis.[18] Postmarketing surveillance for all patients prescribed with leflunomide in Japan showed that 80 of 5911 patients developed interstitial pneumonia and that, of these, 27 died, with ILD being judged to be the primary cause of death in at least 18 cases. The incidence of leflunomide-induced ILD and its mortality rate are higher than the corresponding figures in Western countries;[16,17,19,20] however, the mechanism governing this racial difference for susceptibility to drug-induced ILD is unknown.

In this study, we examined the EMT-inducing abilities of drugs known to cause ILD clinically. Our results showed that A771726, an active metabolite of leflunomide, induces EMT-like phenotypes in cultured human type II alveolar (A549) cells through the inhibition of DHODH. We also provide evidence that administration of leflunomide stimulates bleomycin-induced EMT-like phenomenon in the pulmonary tissue and exacerbates bleomycin-induced pulmonary fibrosis. On the basis of these findings, we consider that leflunomide-induced pulmonary fibrosis involves EMT of lung epithelial cells and that this leflunomide-dependent exacerbation of bleomycin-induced pulmonary fibrosis provides a suitable animal model of drug-induced ILD.

Results

Induction of EMT-like phenotypes by an active metabolite of leflunomide *in vitro*. We first set out to examine the *in vitro* EMT-inducing abilities of drugs known, to induce ILD clinically. As one of the phenotypes related to EMT is growth inhibition,[21] we initially determined the concentration of each drug (A771726 (an active metabolite of leflunomide), amiodarone, methotrexate, imatinib and gefitinib) that led to the suppression of A549 cell growth (Supplementary Figure S1a). Upregulation of the expression of myofibroblast marker proteins (such as α-smooth muscle actin (α-SMA) and collagen I) and downregulation of the expression of epithelial cell marker proteins (such as E-cadherin and precursor of surfactant protein C (proSP-C)) can be used to monitor EMT. Treatment of cells with A771726 or methotrexate upregulated the expression of *α-sma* and *col1a1* (one of the genes for collagen I) mRNAs, and downregulated *E-cadherin* mRNA expression (Supplementary Figure S1b). The other drugs tested (amiodarone, imatinib and gefitinib) did not significantly affect the expression of these genes, except for the downregulation of *E-cadherin* mRNA expression by gefitinib (Supplementary Figure S1b). Immunoblotting analysis showed that protein expression of α-SMA or proSP-C and E-cadherin was increased or decreased, respectively, in the presence of A771726 or methotrexate (Supplementary Figure S1c). As these results suggested that both A771726 and methotrexate can induce EMT in A549 cells, we took into consideration the plasma concentrations of these two drugs at clinical doses (see discussion), before selecting A771726 for further experiments.

As shown in Figure 1a and b, the change in the expression of EMT-related genes (proteins) was dependent on the dose of A771726. Immunostaining analysis showed that treatment of A549 cells with A771726 reduced the expression of E-cadherin at the cell periphery and induced the expression of α-SMA in the cytosol (Figure 1c). We also examined the effect of A771726 on EMT-like phenotypes in primary cultured rat alveolar epithelial cells. As shown in Figure 2a–c, A771726-dependent upregulation or downregulation of the expression of α-SMA and collagen or E-cadherin and proSP-C, respectively, was also observed in primary cultured rat alveolar epithelial cells, although such alteration was observed with lower concentration of A771726 in primary cultured rat alveolar epithelial cells than in A549 cells.

We also examined the effect of A771726 on other EMT-related phenotypes, including an increase in cell migration activity and the activity and expression of MMPs and TIMPs. As shown in Figure 1d, treatment of cells with A771726 stimulated the migration activity of A549 cells. The band intensity based on gelatin zymography, indicative of MMP-2 and MMP-9 activity, was also increased by treatment of cells with A771726 (Figure 1e). The level of TIMP-1 in the culture medium increased in the presence of A771726 (Figure 1f) Furthermore, the expression of *mmp-2*, *mmp-9* and *timp-1* mRNAs was upregulated (Figure 1g). Taken together, these findings support the idea that A771726 induces EMT in A549 cells.

Involvement of Smad-interacting protein 1 and the Notch-signaling pathway in A771726-induced EMT-like phenotypes. A number of transcription factors (such as Snail, Twist, Smad-interacting protein 1 (SIP1) and Slug) are involved in the induction of EMT.[22] As shown in Figure 3a, treatment of cells with A771726 upregulated mRNA expression of SIP1 and Slug and, to a lesser extent, Twist. A771726-dependent upregulation of expression of SIP1 and Slug was also observed at the protein level (Figure 3b). Thus, we tested the contribution of SIP1 to A771726-induced EMT-like phenotypes using its siRNA (unfortunately, we could not obtain siRNA that efficiently suppresses the

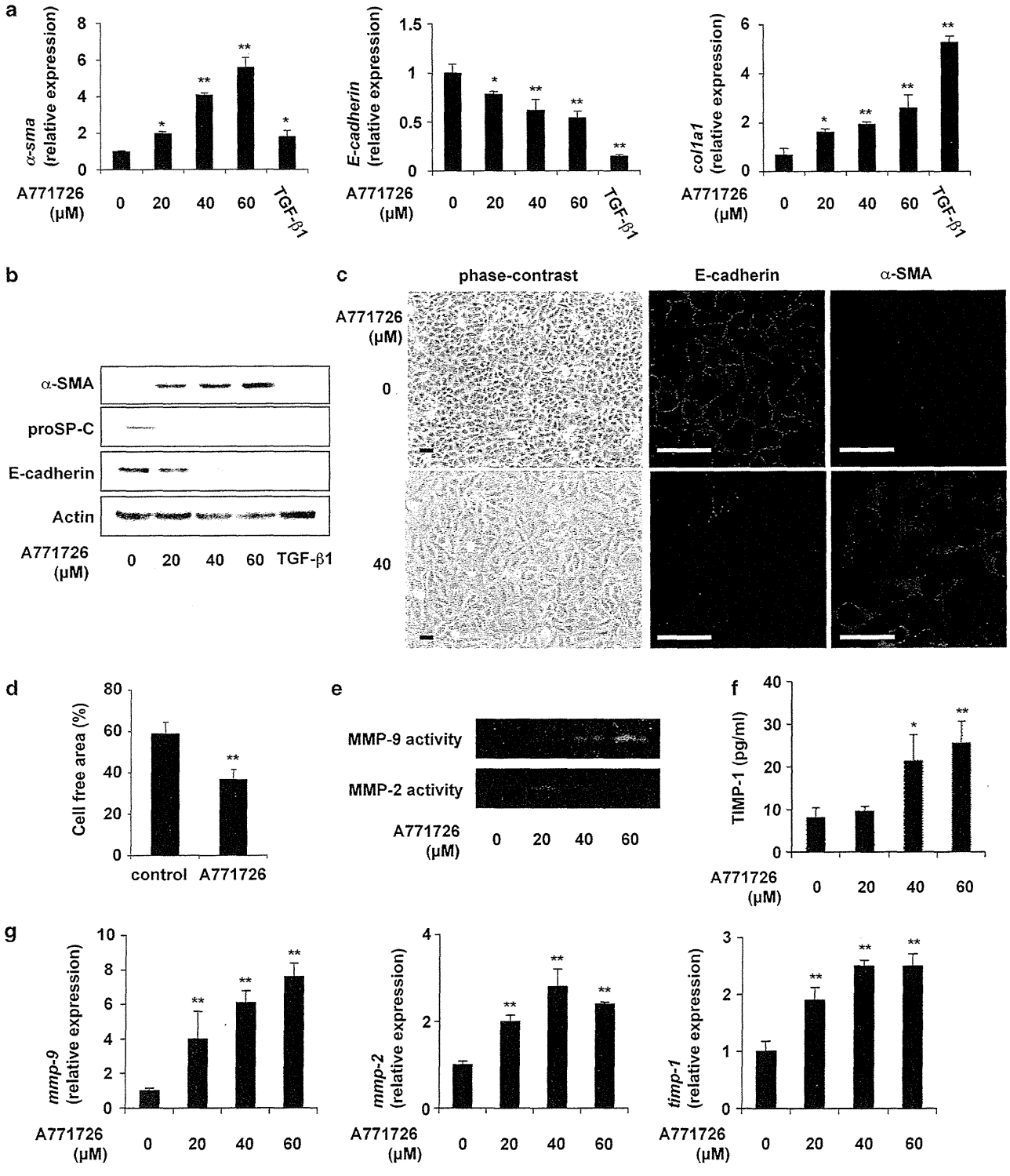

Figure 1 Induction of EMT-like phenotypes by A771726. A549 cells were incubated with the indicated concentration (**a**, **b**, **e**–**g**) or 40 μM (**c**, **d**) of A771726 or 1 ng/ml TGF-β1 (panels a, b) for 48 h (panels a, g) or 96 h (panels b–f). (Panels a, g) Total RNA was extracted and subjected to real-time RT-PCR using a specific primer set for each gene. Values were normalized to the *actin* gene, expressed relative to the control sample. (Panel b) Whole-cell extracts were analyzed by immunoblotting with an antibody against α-SMA, proSP-C, E-cadherin or actin. (Panel c) Morphological changes in the cells were examined by phase-contrast microscopic observation and immunostaining with an antibody against E-cadherin or α-SMA (scale bar, 50 μm). (Panel d) After making wounds, the cells were incubated for 24 h without each drug. The cell-free area was measured and expressed relative to that before the incubation. (Panel e) MMP-9 and MMP-2 activity in the culture medium was measured as described in the 'Materials and Methods' section. (Panel f) The level of TIMP-1 in the culture medium was determined by ELISA. Values shown are mean ± S.D. ($n=3$). $^*P<0.05$; $^{**}P<0.01$ (panels a, d, f, g)

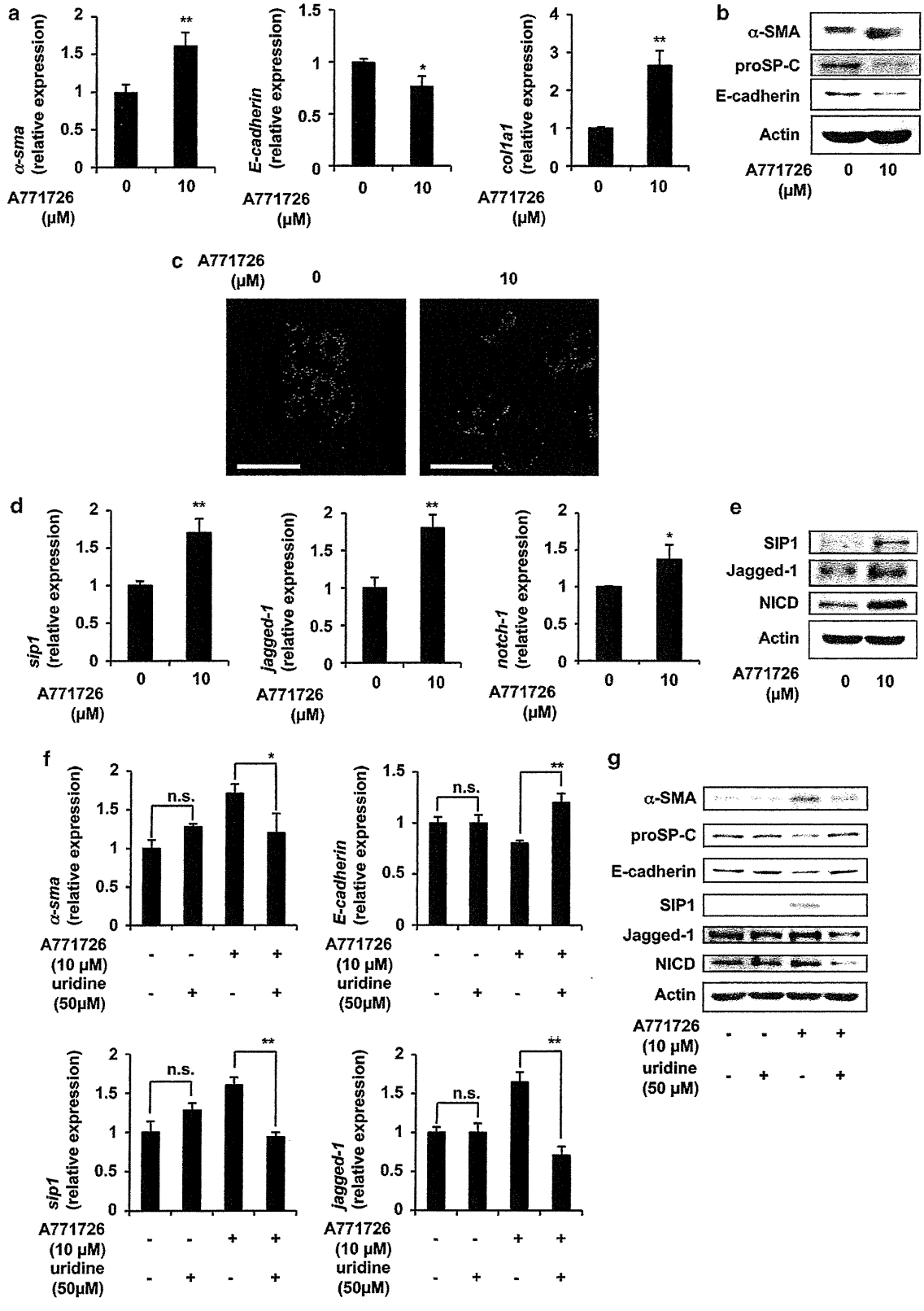

Figure 2 Induction of EMT-like phenotypes by A771726 in primary cultured rat alveolar epithelial cells. Primary cultured rat alveolar epithelial cells were incubated with the indicated concentration of A771726 for 24 h in the absence (**a–e**) or presence (**f**, **g**) of 50 μM uridine. (Panels a, b, d–g) mRNA and protein expression were monitored and expressed as described in the legend of Figure 1. (Panel c) Immunostaining with antibodies against α-SMA (red) and proSP-C (green) (scale bar, 50 μm) was carried out as described in the 'Materials and Methods' section. Values shown are mean ± S.D. ($n=3$). *$P<0.05$; **$P<0.01$; n.s., not significant (panels a, d, f)

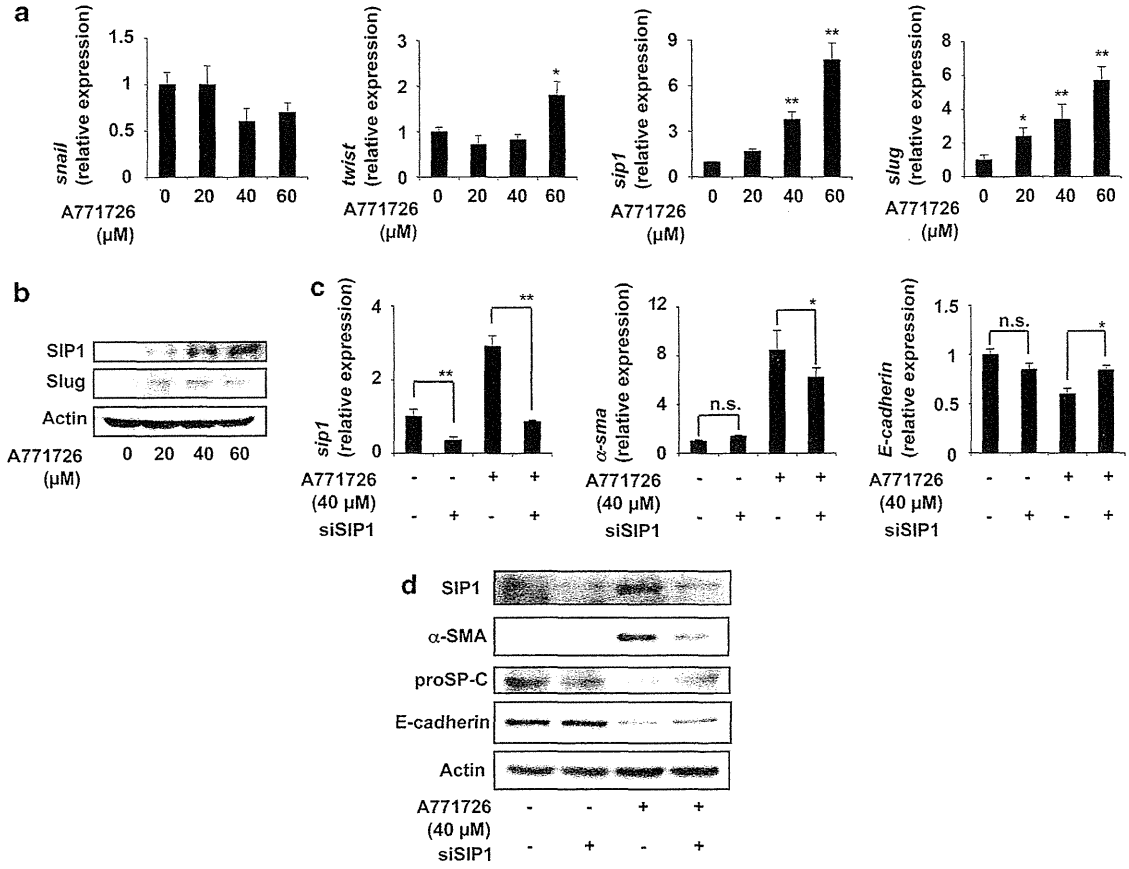

Figure 3 Effect of siRNA for SIP1 on A771726-induced EMT-like phenotypes. (**a**, **b**) A549 cells were incubated with the indicated concentrations of A771726 for 48 h (panel a) or 96 h (panel b). (**c**, **d**) A549 cells were transfected with siRNA for SIP1 (siSIP1 +) or nonspecific siRNA (siSIP1−). After 24 h, the cells were incubated with A771726 (40 μM) for 48 h (panel c) or 96 h (panel d). (Panels a–d) Protein and mRNA expressions were monitored and expressed as described in the legend of Figure 1. Values shown are mean ± S.D. ($n=3$). *$P<0.05$; **$P<0.01$; n.s., not significant

expression of Slug). Transfection of SIP1 siRNA suppressed the expression of *sip1* mRNA and SIP1 protein in both the presence and the absence of A771726 treatment (Figure 3c and d). This transfection partially suppressed the A771726-induced upregulation of α-SMA expression and the downregulation of E-cadherin and proSP-C expression (Figure 3c and d), suggesting that the upregulation of SIP1 expression is at least partly involved in A771726-induced EMT-like phenotypes. A771726-dependent upregulation of expression of SIP1 was also observed in primary cultured rat alveolar epithelial cells (Figure 2d and e).

It has also been reported that TGF-β_1 upregulates the expression of EMT-related transcription factors, including SIP1.[23,24] However, as shown in Supplementary Figure S2a and b, A771726 did not significantly affect the mRNA expression of TGF-β_1 or the level of TGF-β_1 in the culture medium. Furthermore, LY364947, an inhibitor for TGF-β receptor kinase, suppressed the changes in the expression of α-SMA, E-cadherin and proSP-C in the presence of TGF-β_1 but not A771726 (Supplementary Figure S2c and d). It therefore appears that A771726-induced EMT-like phenotypes do not involve modulation of expression and activity of TGF-β_1.

Next, we tested the contribution of the Notch-signaling pathway to A771726-induced EMT-like phenotypes. This pathway, which is triggered by the binding between Notch receptors (Notch-1–4) and ligands (such as Jagged-1, 2 and Delta-like 1 (Dll-1)), is mediated by two proteolytic cleavage events involving the Notch receptor.[25] The second cleavage is catalyzed by γ-secretase, leading to secretion of the Notch intracellular domain (NICD), which then translocates to the nucleus to promote transcription of downstream genes.[26] It was recently reported that activation of the Notch-signaling pathway induces EMT.[27,28] As shown in Figure 4a and b, treatment of cells with A771726 upregulated the expression of *jagged-1*, *2*, *dll-1* and *notch-1*, *3*, *4* mRNAs and Jagged-1 and Dll-1 in a dose-dependent manner. Furthermore, the level of NICD in the nuclear extract was increased in the presence of A771726 and this increase was suppressed by cotreatment with an inhibitor of γ-secretase, *N*-[*N*-(3,5-difluorophenacetyl-L-alanyl)]-*S*-phenylglycine *t*-butyl ester (DAPT) (Figure 4c), suggesting that the Notch-signaling pathway is activated by A771726. To test an idea that the Notch-signaling pathway is involved in A771726-induced EMT-like phenotypes, we examined the effect of DAPT on A771726-induced EMT-like phenotypes. As shown in Figure 4d and e, A771726-induced

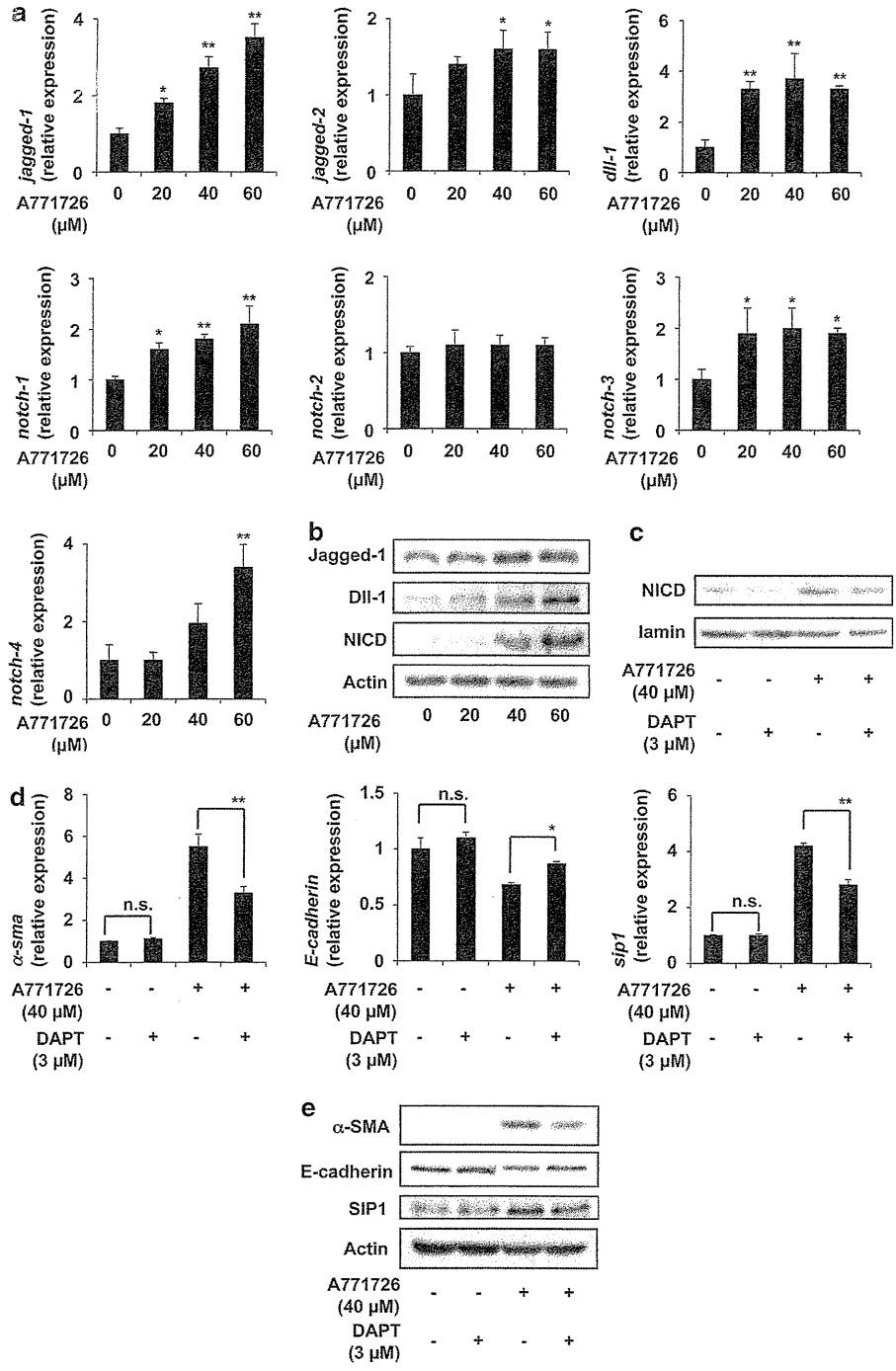

Figure 4 Involvement of the Notch-signaling pathway in A771729-induced EMT-like phenotypes. (**a**, **b**) A549 cells were incubated with the indicated concentrations of A771726 for 48 h (panel a) or for 96 h (panel b). (**c–e**) A549 cells were preincubated with or without DAPT (3 μM) for 1 h and further incubated with or without A771726 (40 μM) for 48 h (panels c, d) or 96 h (panel e) in the presence of the same concentrations of DAPT as in the preincubation step. (Panels a, b, d, e) mRNA and protein expression was monitored and expressed as described in the legend of Figure 1. (Panel c) Nuclear extracts were prepared and analyzed by immunoblotting with an antibody against NICD or lamin. Values shown are mean ± S.D. ($n=3$). *$P<0.05$; **$P<0.01$; n.s., not significant

alterations in the mRNA and protein expression of α-SMA, E-cadherin and SIP1 were partially suppressed by DAPT, suggesting that the Notch-signaling pathway does contribute to A771726-induced EMT-like phenotypes. A771726-dependent upregulation of expression of *jagged-1* and *notch-1* mRNAs and Jagged-1 and NICD was also observed in primary cultured rat alveolar epithelial cells (Figures 2d and e).

To test whether the inhibition of DHODH is involved in the EMT-inducing activity of A771726, we first examined the effect of siRNA for DHODH on the expression of EMT-related genes.

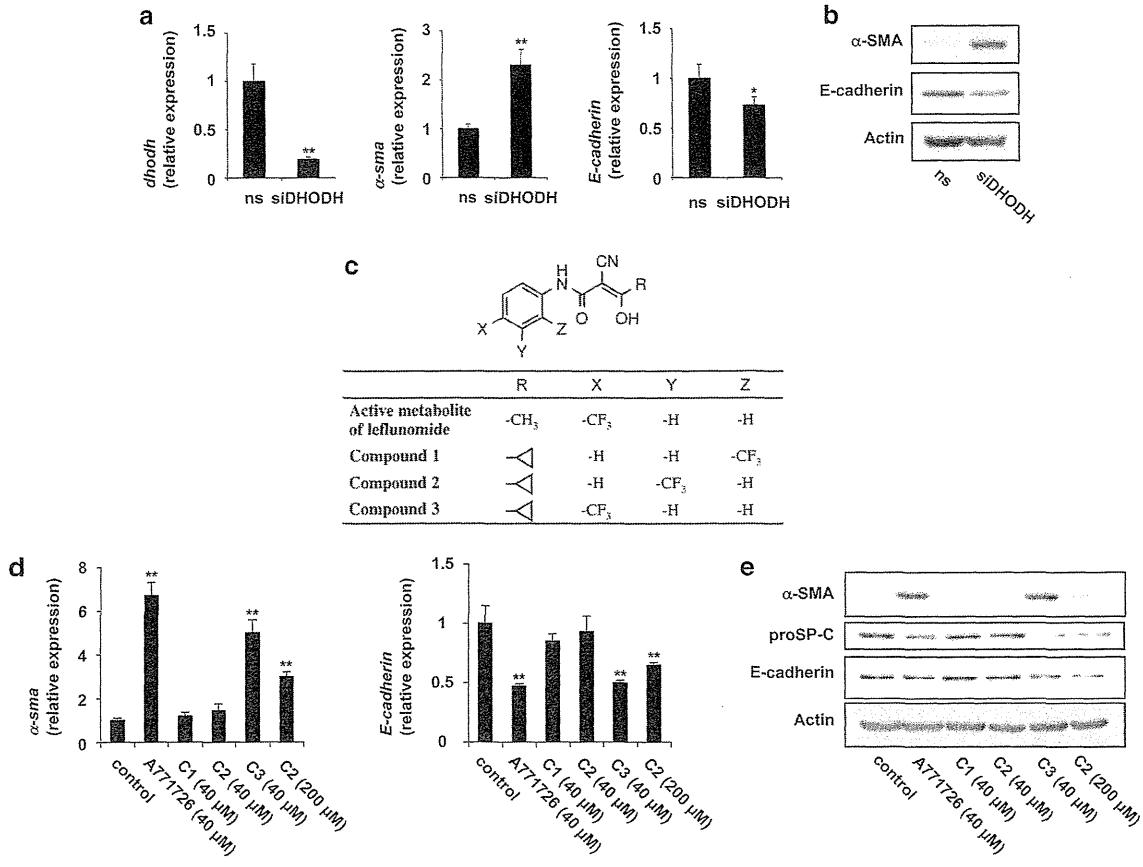

Figure 5 Involvement of DHODH inhibition in A771729-induced EMT-like phenotypes. (**a**, **b**) A549 cells were transfected with siRNA for DHODH (siDHODH) or nonspecific siRNA (ns) for 72 h. (**d**, **e**) A549 cells were incubated with the indicated concentration of each compound for 48 h (panel d) or 96 h (panel e). (Panels a, b, d, e) Protein and mRNA expressions were monitored and expressed as described in the legend of Figure 1. The chemical structures of the compounds are shown in **c**. Values shown are mean ± S.D. ($n=3$). $^*P<0.05$; $^{**}P<0.01$

Transfection of siRNA for DHODH altered the mRNA and protein expression of α-SMA and E-cadherin (Figure 5a and b). A number of A771726 analogs have been synthesized, and their ability to inhibit DHODH was revealed.[29] The DHODH-inhibitory ability of compound 3 is similar to that of A771726; however, that of compound 2 is markedly less, and compound 1 is inert in this context.[29] As illustrated in Figure 5d and e, compound 3 induced EMT-like phenotypes to a similar extent to that observed with A771726. Compound 2 also induced EMT-like phenotypes, but only at a higher concentration, whereas compound 1 had no effect (Figure 5d and e). Taken together, these results suggest that A771726 induces EMT-like phenotypes through inhibition of DHODH.

We further examined the effect of supplementing the cultures with exogenous uridine. As shown in Figure 6a and b, the addition of uridine to the culture medium suppressed the A771726-induced EMT-like phenotypes. Furthermore, it also suppressed the A771726-induced upregulation of expression of *sip1*, *notch-1* and *jagged-1* mRNAs and SIP1, NICD and Jagged-1 (Figure 6a and b). Uridine-dependent suppression of A771726-induced EMT-like phenotypes was also observed in primary cultured rat alveolar epithelial cells (Figure 2f and g). These results further support the notion that A771726 induces EMT-like phenotypes through inhibition of DHODH.

We also found that the addition of cytidine suppressed A771726-induced EMT-like phenotypes (data not shown). As it is known that uridine and cytidine can be synthesized from each other,[30] it seems that these phenotypes are mediated through depletion of the intracellular pool of pyrimidine.

Therefore, we next tested whether the induction of EMT-like phenotypes is specific for inhibition of pyrimidine synthesis or can be observed with inhibition of purine synthesis using 6-mercaptopurine (6-MP), an inhibitor of purine synthesis.[30] Treatment of A549 cells with 100 μM 6-MP inhibited cell growth to a similar extent to that observed with 40 μM A771726 (data not shown). As shown in Figure 6c, treatment of cells with 100 μM 6-MP upregulated the expression of *α-sma* mRNA and downregulated the expression of *E-cadherin* mRNA. However, 6-MP had no effect on the expression of *sip1* and *notch-1* mRNAs and protein expression of α-SMA, SIP1, NICD and proSP-C, and downregulated the expression of *jagged-1* mRNA and Jagged-1 (Figure 6c and d), suggesting that inhibition of pyrimidine synthesis rather than purine synthesis preferentially induces EMT-like phenotypes.

Effect of leflunomide on bleomycin-induced pulmonary fibrosis. As described in the 'Introduction' section, induction

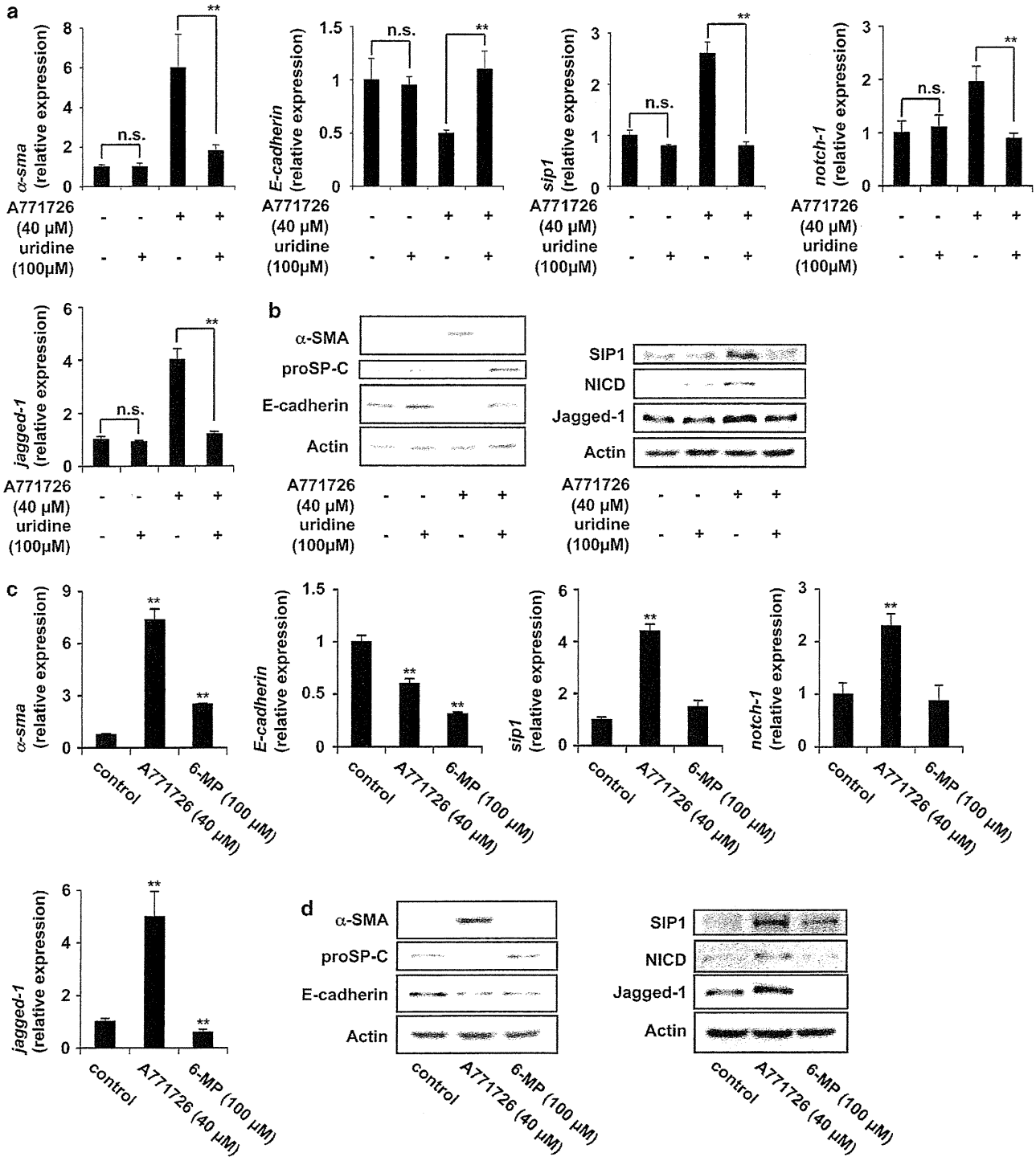

Figure 6 Involvement of inhibition of pyrimidine synthesis in A771729-induced EMT-like phenotypes. A549 cells were incubated with the indicated concentrations of A771726 (**a–d**), uridine (panels a, b) and 6-MP (panels c, d) for 48 h (panels a, c) or 96 h (panels b, d). Protein and mRNA expressions were monitored and expressed as described in the legend of Figure 1. Values shown are mean ± S.D. ($n = 3$). $^{**}P < 0.01$

of EMT of lung epithelial cells has an important role in pulmonary fibrosis, with the *in vitro* results outlined above implicating leflunomide in this process. To investigate this further, we first examined whether EMT is induced in the mouse lung by oral administration of leflunomide alone, finding no significant effect at concentrations of up to 100 mg/kg (data not shown). Next, we tested the idea that leflunomide stimulates EMT-like phenomenon in the presence of other fibrosis-inducing stimuli, such as bleomycin. A once-only (at day 0) intratracheal administration of bleomycin (5 mg/kg)

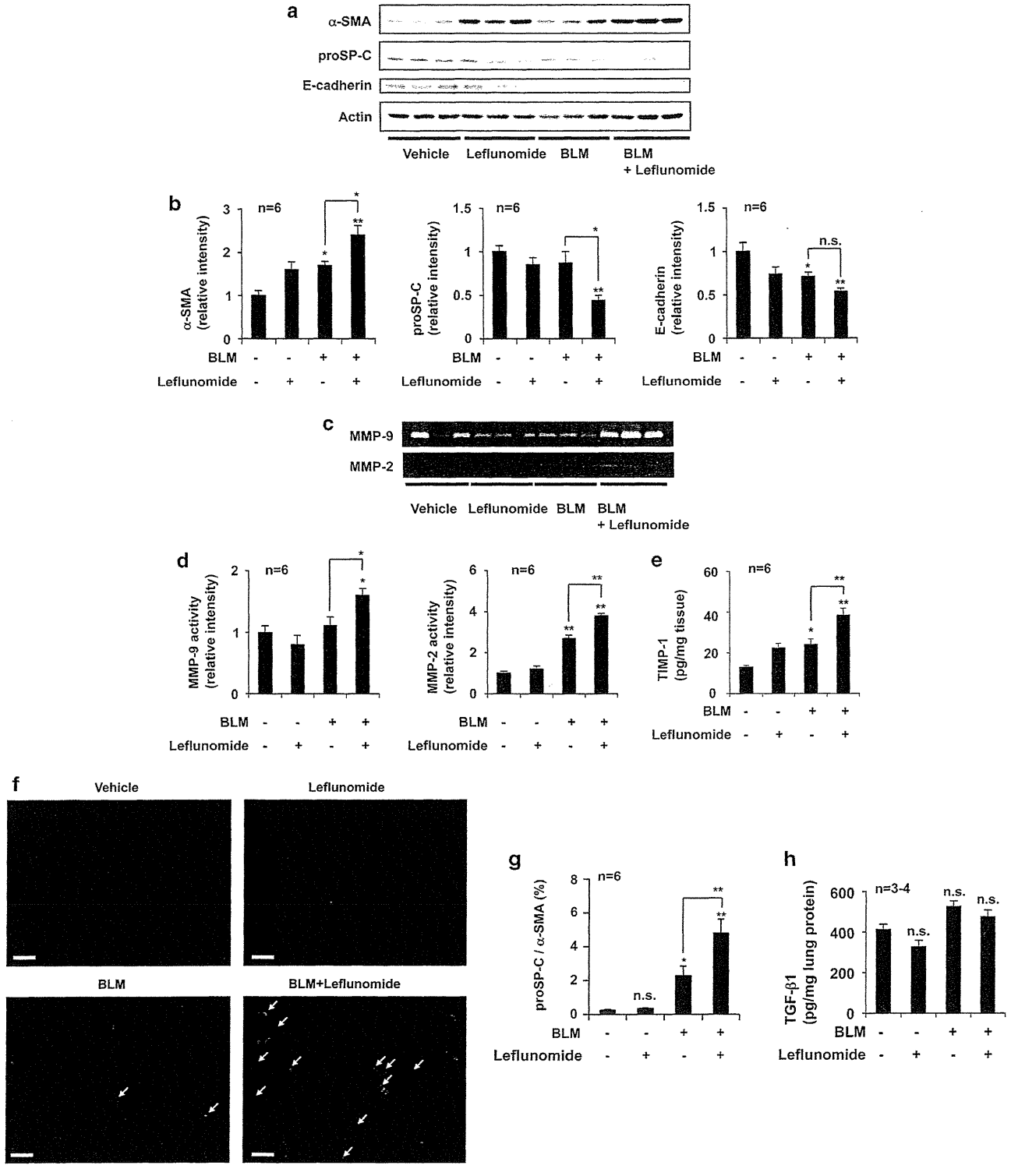

Figure 7 Induction of EMT-like phenotypes by administration of bleomycin and leflunomide. (**a–h**) Mice were treated once only with or without 0.5 mg/kg bleomycin (BLM) (day 0), then orally administered leflunomide (40 mg/kg) or vehicle once per day for 9 days (from day 5 to day 14). (Panel a) Total protein was extracted from pulmonary tissues at day 14 and analyzed with immunoblotting with an antibody against α-SMA, proSP-C, E-cadherin or actin. (Panel b) The intensity of the band of α-SMA, proSP-C and E-cadherin was determined (one of two gels is shown in panel a) and expressed relative to the results obtained in control mice ($n=6$). (Panel c) The activity of MMP-9 and MMP-2 in pulmonary tissues at day 14 was measured as described in the legend of Figure 1. (Panel d) the clear band intensity was determined (one of two gels is shown in panel c) and expressed relative to the control ($n=6$). (Panel e) The level of TIMP-1 in pulmonary tissues at day 14 was determined by ELISA ($n=6$). (Panel f) Sections of pulmonary tissues were prepared at day 14 and subjected to immunohistochemical analysis with an antibody against α-SMA (red) and proSP-C (green) (scale bar, 50 μm). (Panel g) The ratio of EMT-induced cells (coexpression of α-SMA and proSP-C) to total cells (500–800 cells) was determined ($n=6$). (Panel h) The level of TGF-β1 in pulmonary tissue at day 14 days was determined by ELISA ($n=3$–4). Values are mean ± S.E.M. $^*P<0.05$; $^{**}P<0.01$; n.s., not significant

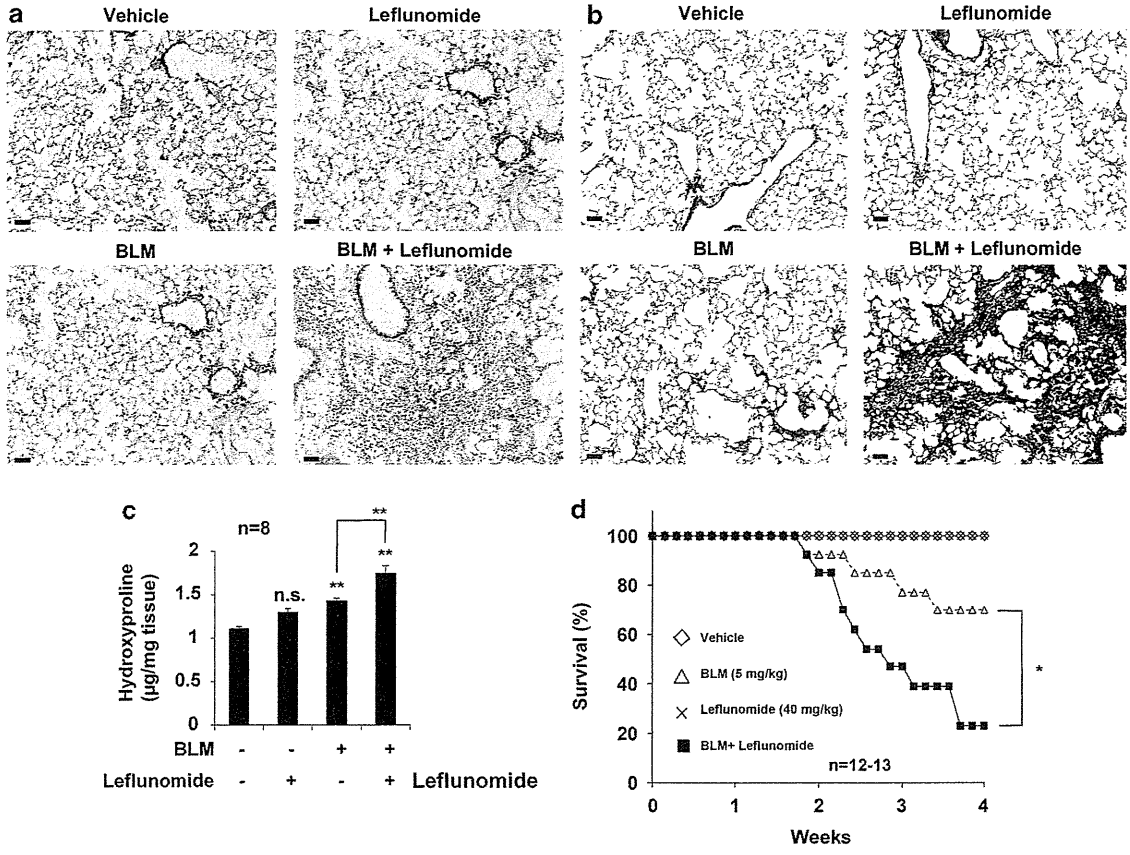

Figure 8 Effect of leflunomide on bleomycin-induced pulmonary fibrosis. (**a–c**) Mice were treated once only with or without 0.5 mg/kg bleomycin (BLM) (day 0), then orally administered leflunomide (40 mg/kg) or vehicle once per day for 9 days (from day 5 to day 14). (Panels a, b) Sections of pulmonary tissue were prepared at day 14 and subjected to histological examination (H & E staining (panel a) or Masson's trichrome staining (panel b)) as described in the 'Materials and Methods' section (scale bar, 50 μm). (Panel c) The pulmonary hydroxyproline level at day 14 was determined as described in the 'Materials and Methods' section ($n=8$). (**d**) Mice were treated once only with BLM (5 mg/kg) at day 0 and were then orally administered leflunomide (40 mg/kg) once per day for 3 weeks (from day 7 to day 28). The survival rate of the animals was monitored ($n=12$–13). Values are mean ± S.E.M. $^*P<0.05$; $^{**}P<0.01$; n.s., not significant

induced apparent EMT-like phenomenon 14 days after treatment (see below). To examine the effect of leflunomide on the bleomycin-induced EMT-like phenomenon, we used a lower dose of bleomycin (0.5 mg/kg). Immunoblotting analysis of pulmonary tissues revealed that administration of bleomycin alone at this dose slightly increased or decreased the level of α-SMA or E-cadherin and proSP-C, respectively, an effect that was further stimulated by simultaneous administration of leflunomide (40 mg/kg), although the results were not always statistically significant (Figure 7a and b). We also measured MMP activity and the level of TIMP-1 by gelatin zymography and ELISA, respectively, and found that these were slightly elevated in response to administration of bleomycin alone, an effect that was further stimulated by simultaneous administration of leflunomide (Figure 7c–e), overall suggesting that leflunomide stimulates bleomycin-induced EMT-like phenomenon.

To test this idea further, we then used immunohistochemical analysis to detect cells with positive expression of both α-SMA and proSP-C, a marker of EMT of lung epithelial cells.[14] As shown in Figure 7f and g, a few double-positive cells were detected in lung sections prepared from bleomycin-treated mice; this number being dramatically increased by simultaneous administration of leflunomide. Administration of leflunomide alone had no such effect (Figure 7f and g).

We next measured the pulmonary level of TGF-β1 and found that administration of bleomycin (0.5 mg/kg) and leflunomide, either alone or in combination had no significant effect (Figure 7h). Administration of bleomycin (0.5 mg/kg) and leflunomide also did not affect the pulmonary level of connective tissue growth factor (CTGF) (Supplementary Figure S3).

We then examined the effect of administration of leflunomide on bleomycin-induced pulmonary fibrosis by monitoring histopathological changes and pulmonary hydroxyproline levels (an indicator of collagen levels). Histopathological analysis of pulmonary tissue using hematoxylin and eosin staining showed that the simultaneous administration of leflunomide (40 mg/kg) and bleomycin (0.5 mg/kg) induced severe pulmonary damage (thickened and edematous alveolar walls and interstitium, and infiltration of leucocytes) (Figure 8a). Administration of either leflunomide or bleomycin alone did not cause such clear pulmonary damage (Figure 8a). Masson's trichrome staining of collagen revealed that administration of bleomycin caused slight collagen deposition, an effect, which was greatly exacerbated by

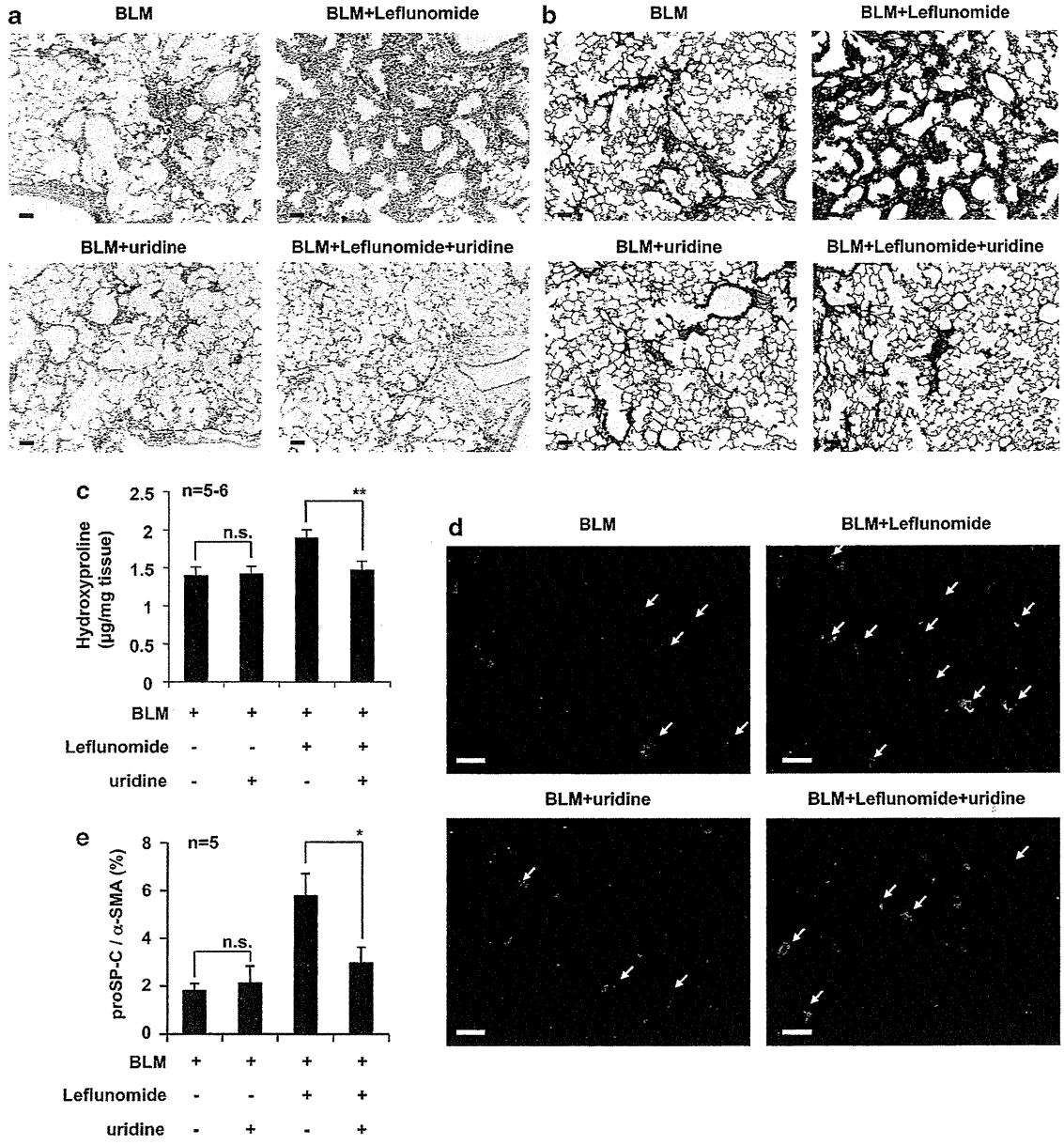

Figure 9 Effect of coadministration of uridine on leflunomide-induced exacerbation of pulmonary fibrosis and EMT-like phenotypes. (**a–c**) Mice were treated once only with or without 0.5 mg/kg bleomycin (BLM) (day 0), then administered leflunomide (40 mg/kg) and uridine (50 mg/kg) once per day for 9 days (from day 5 to day 14). (Panels a, b) Sections of pulmonary tissue were prepared at day 14 and subjected to histological examination as described in the legend of Figure 8 (scale bar, 50 μm). (Panel c) The pulmonary hydroxyproline level was determined at day 14 as described in the legend of Figure 8 ($n=5$–6). (**d, e**) Immunohistochemical analysis was performed as described in the legend of Figure 7 (scale bar, 50 μm) ($n=5$). Values are mean ± S.E.M. $^{**}P<0.01$; $^{*}P<0.05$; n.s., not significant

simultaneous administration of leflunomide (Figure 8b). The pulmonary hydroxyproline level was slightly increased by administration of bleomycin alone, but this effect was further enhanced by simultaneous administration of leflunomide (Figure 8c). These results suggest that administration of leflunomide exacerbates bleomycin-induced pulmonary fibrosis.

We next examined the effect of leflunomide on the survival of mice treated with bleomycin. As shown in Figure 8d, administration of bleomycin alone caused death, the rate of which was accelerated by simultaneous administration of leflunomide.

To test whether leflunomide exacerbates bleomycin-induced pulmonary fibrosis through inhibition of DHODH, we examined the effect of coadministration of uridine. As shown in Figure 9a–c, coadministration of uridine clearly suppressed pulmonary tissue damage, collagen deposition and increases in pulmonary hydroxyproline levels observed in mice treated with both bleomycin and leflunomide. We also found a decrease in the number of cells expressing both α-SMA and proSP-C in mice that had been coadministered uridine (Figure 9d and e). These findings suggest that the exacerbation of bleomycin-induced pulmonary fibrosis by

leflunomide is mediated by its inhibitory effect on DHODH and resulting stimulation of bleomycin-induced EMT-like phenomenon.

Discussion

Although drug-induced ILD, particularly interstitial pneumonia associated with pulmonary fibrosis, is a serious clinical concern, the molecular mechanism governing this phenomenon is unknown, leading to the lack of a suitable animal model. Consequently, neither a clinical protocol for the treatment of drug-induced ILD nor an assay system to eliminate candidate drugs with the potential to cause this type of side effect has been established. A number of previous reports have suggested that cytotoxic and allergy-inducing effects of the drugs are involved in drug-induced ILD.[3–5,19] In this study, for the first time, we focused on the EMT of lung epithelial cells in a bid to understand the mechanism of drug-induced ILD (pulmonary fibrosis).

When we examined the EMT-inducing abilities of drugs known to induce ILD clinically, we found that A771726 and methotrexate produced EMT-like phenotypes. The concentration of methotrexate used was much higher than its plasma concentration at a clinical dose (approximately 0.01–0.2 μM).[31] On the other hand, A771726 induced EMT-like phenotypes at concentrations similar to those obtained in the plasma when administered at therapeutic levels (approximately 40–350 μM).[32] Thus, we considered that induction of EMT-like phenotypes by A771726 is clinically relevant and investigated the underlying molecular mechanism. Studies on other cell types have shown that A771726 induces apoptosis and diminishes proliferation in myeloma cells[33] and inhibits proliferation and collagen synthesis and induces apoptosis in hepatic stellate cells,[34] suggesting that A771726 affects cell physiology differently depending on cell-type species.

Among the transcription factors known to induce EMT, we found that both SIP1 and Slug mRNA expression was upregulated by A771726 and that transfection of cells with siRNA for SIP1 partially suppressed the A771726-induced EMT-like phenotypes, suggesting that SIP1 has a role in this phenomenon. However, although it is well known that TGF-β1 induces EMT through transcription factors that include SIP1,[23] the lack of involvement of the TGF-β-signaling pathway was suggested by the fact that (1) TGF-β1 expression and the level of TGF-β1 in the culture medium were not affected by A771726 and (2) an inhibitor of the TGF-β-signaling pathway did not affect the A771726-induced EMT-like phenotypes. This led us to investigate the involvement of the Notch-signaling pathway, which has recently been reported to have an important role not only in EMT but also in pulmonary fibrosis.[27,35] Expression of some Notch ligands and receptors was upregulated by A771726, and an inhibitor for this pathway (DAPT) partially suppressed the A771726-induced EMT-like phenotypes, suggesting the involvement of the Notch-signaling pathway to this phenomenon. Furthermore, although it is known that A771726 has various activities other than inhibition of DHODH, including inhibition of tyrosine kinase and cyclooxygenase-2,[36,37] we clearly showed that the primary target of A771726 for induction of EMT is DHODH based on the following observations: (1) transfection of cells with siRNA for DHODH induced EMT-like phenotypes, (2) among the A771726 analogs, the ability to induce EMT-like phenotypes correlated with the ability to inhibit DHODH and (3) the addition of uridine to the culture medium completely suppressed the A771726-induced EMT-like phenotypes. However, how inhibition of DHODH causes EMT remains unclear.

We found that administration of leflunomide alone did not induce EMT-like phenomenon in mouse lung. As one of the risk factors for leflunomide-induced ILD is preexisting pulmonary fibrosis,[20,38] we hypothesized that leflunomide stimulates EMT-like phenotypes in the presence of other fibrosis-inducing stimuli. In fact, we found that the administration of leflunomide stimulated bleomycin-induced EMT-like phenotypes in the mouse lung, an effect which was suppressed by coadministration of uridine. This is the first demonstration that administration of a drug known to induce ILD clinically modulates EMT-like phenotypes *in vivo*. We also found that administration of leflunomide stimulated bleomycin-induced pulmonary fibrosis, and that this was suppressed by co-administration of uridine. Taken together, our findings suggest that leflunomide exacerbates bleomycin-induced pulmonary fibrosis through inhibition of DHODH and the resulting induction of EMT in lung epithelial cells. As described in the 'Introduction' section, lung myofibroblasts are produced by both activation of lung fibroblasts and EMT of lung epithelial cells.[9] We found that A771726 did not affect the expression of α-SMA and collagen I in HFL1 (human lung fibroblast) cells (data not shown), suggesting that A771726 does not activate fibroblasts to form myofibroblasts.

These results suggest that the EMT-inducing ability of leflunomide is involved in its exacerbation of pulmonary fibrosis. This finding is an important step toward addressing the molecular mechanism of drug-induced ILD, as well as the mechanism governing the racial differences for susceptibility to ILD induced by the drug. It is possible that the susceptible phenotype of Japanese patients is due to a specific polymorphism in genes related to EMT. Furthermore, the exacerbation of pulmonary fibrosis by leflunomide can be used as an animal model of drug-induced pulmonary fibrosis, allowing screening to eliminate candidate drugs for the potential side effects.

Materials and Methods

Chemicals and animals. Paraformaldehyde, fetal bovine serum (FBS), 4-(dimethylamino)-benzaldehyde (DMBA), chloramine T, Orange G, uridine, 6-MP, LY364947 and an antibody against α-SMA were obtained from Sigma (St. Louis, MO, USA). TGF-β1 was acquired from Funakoshi Co. (Tokyo, Japan). Bleomycin was purchased from Nippon Kayaku (Tokyo, Japan). DAPT was from the Peptide Institute Inc. (Tokyo, Japan). ELISA kits for TGF-β1 and TIMP-1 were obtained from R&D Systems Inc. (Minneapolis, MN, USA). The RNeasy kit and HiPerFect were obtained from Qiagen (Valencia, CA, USA), the PrimeScript first-strand cDNA Synthesis Kit was from Takara Bio (Ohtsu, Japan), and the iQ SYBR Green Supermix was from Bio-Rad Laboratories (Hercules, CA, USA). Antibodies against SIP1, jagged-1, Dll-1, Notch-1, actin and lamin were purchased from Santa Cruz Biotechnology Inc. (Santa Cruz, CA, USA) and that against E-cadherin was from Zymed Laboratories (San Francisco, CA, USA). An antibody against proSP-C was from Millipore Co. (Bedford, MA, USA) and that against Slug was from Cell Signaling (Bedford, MA, USA). Alexa Fluor 594 (or 488) goat anti-mouse IgG and Alexa Fluor 488 goat anti-rabbit IgG were obtained from Invitrogen (Carlsbad, CA, USA). Mounting medium for immunohistochemical analysis (VECTASHIELD) was from Vector Laboratories (Burlingame, CA, USA). Cytospin 4 was purchased from